

This is an Open Access document downloaded from ORCA, Cardiff University's institutional repository:<https://orca.cardiff.ac.uk/id/eprint/143772/>

This is the author's version of a work that was submitted to / accepted for publication.

Citation for final published version:

Westacott, Laura J., Haan, Niels, Evison, Claudia, Marei, Omar, Hall, Jeremy , Hughes, Timothy R. , Zaben, Malik , Morgan, B. Paul , Humby, Trevor , Wilkinson, Lawrence S. and Gray, William P. 2021. Dissociable effects of complement C3 and C3aR on survival and morphology of adult born hippocampal neurons, pattern separation, and cognitive flexibility in male mice. *Brain, Behavior, and Immunity* 98 , pp. 136-150. 10.1016/j.bbi.2021.08.215

Publishers page: <http://dx.doi.org/10.1016/j.bbi.2021.08.215>

Please note:

Changes made as a result of publishing processes such as copy-editing, formatting and page numbers may not be reflected in this version. For the definitive version of this publication, please refer to the published source. You are advised to consult the publisher's version if you wish to cite this paper.

This version is being made available in accordance with publisher policies. See <http://orca.cf.ac.uk/policies.html> for usage policies. Copyright and moral rights for publications made available in ORCA are retained by the copyright holders.



1
2 **Dissociable effects of complement C3 and C3aR on survival and**
3 **morphology of adult born hippocampal neurons, pattern**
4 **separation, and cognitive flexibility in male mice.**
5
6

7 Laura J. Westacott^{1,4}, Niels Haan^{1,4}, Claudia Evison⁷, Omar Marei¹, Jeremy Hall^{1,4},
8 Timothy R. Hughes³, Malik Zaben^{1,5}, B. Paul Morgan^{3,4,6}, Trevor Humby^{1,2,4},
9 Lawrence S. Wilkinson^{1,2,4*} & William P. Gray^{1,4,5*†}
10

11 **Author Affiliations**

12
13
14 ¹ Neuroscience and Mental Health Research Institute, MRC Centre for Neuropsychiatric
15 Genetic and Genomics, School of Medicine, Hadyr Ellis Building, Cardiff University, Cardiff,
16 CF24 4HQ, UK.

17 ² Behavioural Genetics Group, Schools of Psychology and Medicine, Cardiff University,
18 Cardiff, CF10 3AT, UK.

19 ³ Complement Biology Group, Systems Immunity Research Institute, School of Medicine,
20 Cardiff University, CF14 4XW, Cardiff UK.

21 ⁴ Hodge Centre for Neuropsychiatric Immunology, School of Medicine, Cardiff University,
22 Cardiff CF24 4HQ, UK.

23 ⁵ Brain Repair and Intracranial Neurotherapeutics (BRAIN), Biomedical Research Unit,
24 Division of Psychological Medicine and Clinical Neurosciences, School of Medicine, Cardiff
25 University, CF24 4HQ, UK.

26 ⁶ UK Dementia Research Institute, Cardiff University, Cardiff, CF24 4HQ, UK.

27 ⁷ National Centre for Mental Health, Hadyr Ellis Building, Cardiff University, Cardiff, CF24
28 4HQ, UK.

29
30
31 *Joint senior authors
32
33

34 †Corresponding Author: Prof William Gray

35 **Email:** GrayWP@cardiff.ac.uk

36 **Address:** Brain Repair and Intracranial Neurotherapeutics (BRAIN), Biomedical
37 Research Unit, Division of Psychological Medicine and Clinical Neurosciences, School
38 of Medicine, Cardiff University, CF24 4HQ, UK.
39
40
41

42 **Key words:** Complement system, adult neurogenesis, morphology, hippocampus,
43 pattern separation, cognitive flexibility
44

45 **Abbreviations:** AHN; adult hippocampal neurogenesis, C3; complement component
46 3, C3aR; complement C3a receptor, GCs; granule cells, GCL; granule cell layer.
47
48
49

Abstract

50
51
52
53
54
55
56
57
58
59
60
61
62
63
64
65
66
67
68
69
70
71
72
73
74

Adult hippocampal neurogenesis (AHN) is a form of ongoing plasticity in the brain that supports specific aspects of cognition. Disruptions in AHN have been observed in neuropsychiatric conditions presenting with inflammatory components and are associated with impairments in cognition and mood. Recent evidence highlights important roles of the complement system in synaptic plasticity and neurogenesis during neurodevelopment and in acute learning and memory processes. In this work we investigated the impact of the complement C3/C3aR pathway on AHN and its functional implications for AHN-related behaviours. In $C3^{-/-}$ mice, we found increased numbers and accelerated migration of adult born granule cells, indicating that absence of C3 leads to abnormal survival and distribution of adult born neurons. Loss of either C3 or C3aR affected the morphology of immature neurons, reducing morphological complexity, though these effects were more pronounced in the absence of C3aR. We assessed functional impacts of the cellular phenotypes in an operant spatial discrimination task that assayed AHN sensitive behaviours. Again, we observed differences in the effects of manipulating C3 or C3aR, in that whilst $C3aR^{-/-}$ mice showed evidence of enhanced pattern separation abilities, $C3^{-/-}$ mice instead demonstrated impaired behavioural flexibility. Our findings show that C3 and C3aR manipulation have distinct effects on AHN that impact at different stages in the development and maturation of newly born neurons, and that the dissociable cellular phenotypes are associated with specific alterations in AHN-related behaviours.

75

76 **1. Introduction**

77 Adult hippocampal neurogenesis (AHN) is a unique process that recapitulates the
78 steps of developmental neurogenesis in an otherwise anti-neurogenic brain, from
79 precursor proliferation, fate specification, migration and differentiation to morphological
80 and synaptic integration of newly born neurons¹. Originating from radial glial cells,
81 neuronal progenitor cells are born in their thousands within the sub granular zone of
82 dentate gyrus². While the majority of these cells undergo programmed cell death within
83 the first few weeks of life³, surviving immature granule cell (GC) neurons progress
84 through a multifaceted developmental process as they mature and integrate into the
85 hippocampal circuitry⁴.

86 The function of AHN has been debated but current evidence suggests it is involved
87 in information processing critical to adaptive behaviour across a number of areas
88 including learning, memory and emotionality⁵⁻⁷. In particular, young adult born neurons
89 are thought to perform pattern separation, the process that enables discrimination of
90 highly similar, overlapping spatial and temporal stimuli, fostering the appropriate
91 separation and storage of similar memory traces or engrams thereby reducing
92 interference^{8,9}. Key evidence supporting a role for AHN in pattern separation comes
93 from studies in which ablation of neurogenesis resulted in specific impairments in
94 discriminating stimuli with a high degree of spatial similarity or overlap, but not stimuli
95 that are more readily distinguished¹⁰⁻¹². Evidence also supports an important role for
96 AHN in cognitive flexibility and the underlying processes of behavioural inhibition that
97 allows flexible responding in the face of changing contingencies⁵, and elements of
98 cognitive flexibility and behavioural inhibition have been shown to be sensitive to
99 experimental manipulations of AHN¹³⁻¹⁷.

100 The process of AHN is subject to regulation by myriad factors, including microglia
101 and immune signalling^{18,19}. The complement system consists of separate activation
102 pathways which converge on a single molecule, C3, and then culminate in the terminal
103 pathway²⁰. It is through C3 activation that the main effectors of the complement system
104 are generated, including the anaphylatoxin C3a. This peptide signals via its cognate G
105 protein-coupled C3a receptor (C3aR) to stimulate intracellular signalling pathways
106 leading to the modulation of critical cellular functions²¹ and pro- and anti-inflammatory
107 actions²². In recent years, prominent roles have emerged for the complement system
108 in brain development, including synapse elimination²³ and embryonic neurogenesis²⁴,
109 but also in neurodegeneration²⁵⁻²⁷ though how complement may influence ongoing
110 neurogenesis and cognitive functions within the adult brain have received relatively
111 little focus. Given converging evidence of aberrant adult neurogenesis^{28,29} and
112 cognitive dysfunction³⁰⁻³² in neuropsychiatric disorders associated with abnormal
113 complement activity^{33,34}, it is important that we improve our understanding of how
114 complement may regulate ongoing neuroplasticity and neurodevelopment in the
115 context of AHN.

116 Previous literature illustrates conflicting roles for different complement pathways
117 in regulating basal AHN. Adult *C3*^{-/-} and *C3aR*^{-/-} mice, and wildtype mice in which C3aR
118 was pharmacologically blocked, showed reduced numbers of adult born neurons³⁵,
119 suggesting that the C3a-C3aR axis is a positive regulator of AHN. In contrast, another
120 report focusing on the role of a different breakdown product of C3, found an inhibitory
121 role of C3d/CR2 signalling in adult neurogenesis, whereby *CR2*^{-/-} mice showed
122 elevated levels of basal neurogenesis in the adult hippocampus³⁶. Therefore, two
123 opposing regulatory roles have been assigned to these separate breakdown products
124 of C3, which suggest both pro and anti-neurogenic properties of the complement

125 system under physiological conditions. Furthermore, the functional consequences of
126 these changes for cognition are unknown. Improved spatial memory recall and reversal
127 learning have been described in *C3*^{-/-} mice^{37,38}, and blockade of the C3a receptor
128 improved cognition in pathological contexts^{26,27,39}, but there have not yet been any
129 direct investigations of AHN-associated cognition in complement knockout models.

130 Other important variables in the neurogenic process include the morphology and
131 functional integration of newborn neurons into the existing hippocampal circuitry⁴⁰. In
132 addition to the aforementioned roles of complement in sculpting neuronal circuitry in
133 the developing brain^{23,41}, several studies have implicated the C3a/C3aR axis in
134 modulating neuronal morphology *in vitro*^{39,42,43}. Whether complement is involved in the
135 morphological maturation of adult born neurons *in vivo* within the hippocampal
136 neurogenic niche has not yet been reported.

137 Using mice constitutively deficient in complement *C3* or *C3aR*, we investigated the
138 impact of these pathways on discrete stages of the neurogenic process occurring in
139 the adult hippocampus. We also assessed behaviour in a translational touch-screen
140 visual discrimination task previously employed to demonstrate the involvement of AHN
141 in pattern separation^{10,12,44}. Our findings reveal different effects of C3 and C3aR
142 manipulation on AHN and related behaviours. Cellular effects of C3aR deficiency were
143 mainly limited to effects on the morphological complexity of adult born neurons, whilst
144 C3 deficiency impacted predominantly on their survival and ultimate location. The
145 dissociations in cellular effects were associated with different behavioural outcomes
146 and together the data suggest cellular mechanisms linking C3aR to pattern separation
147 and C3 to cognitive flexibility, respectively.

148

149

150 **2. Materials and Methods**

151 For full methods, see *Supplementary Information*.

152

153 **2.1 Mouse models and husbandry**

154 Wildtype and $C3^{-/-}$ strains were sourced in-house from Professor B. Paul Morgan and
155 Dr Timothy Hughes (strains originally from The Jackson Laboratory; B6.PL-Thy1^a/CyJ
156 stock#000406 and B6;129S4-C3tm1Crr/J stock#003641 respectively). $C3aR^{-/-}$ mice
157 were provided by Professor Craig Gerard of Boston Children's Hospital, USA (mice
158 subsequently provided to The Jackson Laboratory by Prof. Gerard, strain
159 B6.129S4(C)- $C3ar1^{tm1Cge}$ /BaoluJ). $C3^{-/-}$ and $C3aR^{-/-}$ mice were maintained via
160 homozygous breeding on a C57Bl/6J background and in all experiments were
161 compared to wildtype mice also on a C57Bl/6J background. Male mice were kept in
162 a temperature and humidity-controlled vivarium ($21\pm 2^{\circ}\text{C}$ and $50\pm 10\%$, respectively)
163 with a 12-hour light-dark cycle (lights on at 07:00hrs/lights off at 19:00hrs). For ex vivo
164 histological analyses, animals were between 8 and 12 weeks of age at the time of
165 sacrifice. For behavioural testing, animals were habituated to daily handling by the
166 experimenter for 2 weeks prior to beginning behavioral testing at 8 weeks of age and
167 were approximately 22 weeks of age on completion. All procedures were performed
168 in accordance with the requirements of the UK Animals (Scientific Procedures) Act
169 (1986).

170

171 **2.2 Pulse-chase experiments**

172 Animals were injected with 5-bromo-2'-deoxyuridine (Sigma Aldrich, UK) diluted in
173 sterile Phosphate buffered saline (pH 7.4) at a dose of 100 mg/kg i.p either 6 hours

174 prior to sacrifice (short pulse BrdU) or once daily on 5 consecutive days, with sacrifice
175 30 days after the first dose (long pulse BrdU).

176 **2.3 Tissue sampling and Immunohistochemistry**

177 Paraformaldehyde fixed brain tissue was sectioned on a cryostat, with 6 sections
178 collected per animal, spanning the longitudinal axis of the hippocampus beginning
179 approximately -0.94 mm from bregma and ending at approximately -3.40 mm from
180 bregma ⁴⁵. Sections were selected using a stereological sampling rate of 1/10. Free
181 floating 40µm sections were used for immunohistochemistry (see Supplementary
182 Information).

183 **2.4 Microscopy**

184 Tissue sections were imaged on an upright Leica DM6000B fluorescence microscope
185 using tile scanning at 40x magnification to capture the entire left and right dentate gyri
186 in each section. Experimenters were blinded to genotype during all analyses.

187 **2.5 Cell counting and analyses**

188 In order to estimate the total number of cells (e.g., DCX⁺, BrdU⁺, NeuN⁺) in the whole
189 dentate gyri of each animal, the number of cells counted in the left and right dentate
190 were summed and multiplied by the intersection interval (10) to obtain the total number
191 of cells for the region spanning the current section until the next section. This was
192 repeated for each of 6 sections, and the estimates obtained were summed in order to
193 give a measure of the total number of cells present in the entire DG per animal. For
194 migration analyses, the thickness of the GCL was measured in each section and
195 divided into four equally sized bins, each approximately two cells thick and the first of
196 which represented the sub granular zone (SGZ). The distance of individual BrdU⁺ cells

197 from the inner (hilar) portion of the SGZ was measured using ImageJ and the total
198 number and proportions of cells per bin was calculated.

199 **2.6 Sholl analyses**

200 DCX⁺ cells were systematically randomly sampled and traced using Simple neurite
201 tracer plugin⁴⁶ for ImageJ software (<https://imagej.net/Fiji>). Any cells with processes
202 not entirely visible were excluded from analyses. For each cell, processes were traced
203 manually. Primary and secondary path lengths were extracted, before Sholl analysis
204 was performed. For all experiments detailed, radii separated by a distance of 10 μm
205 were used. We compared sholl profiles using a single metric, the area under the curve
206 (AUC). In addition, we analysed the Branching Index (BI), which produces a value that
207 is proportioned to differences in the pattern of neurite ramification, and is relative to
208 the amount of branches a neurite possesses⁴⁷. Data on primary path lengths
209 (processes emanating directly from the soma) and branches (defined as any process
210 originating from a primary process) was collected in addition to branch numbers.

211 **2.7 Behavioural testing**

212 All behavioural testing was conducted within the light phase. Genotypes were
213 counterbalanced across morning and afternoon testing sessions. For the duration of
214 testing, water was restricted to a two-hour access period per day. Body weight was
215 monitored throughout the period of water deprivation, and animals were maintained at
216 90% of their free-feeding body weight prior to commencing water restriction. All
217 subjects had *ad libitum* access to food in the home-cage throughout the behavioural
218 testing period. All apparatus was cleaned thoroughly in between experimental subjects
219 using 70% ethanol solution to remove odours.

220 **2.7.1 Locomotor activity (LMA)**

221 LMA was assessed in a 120-minute session conducted in the dark within a plexiglas
222 chamber spanned transversely by two infrared beams.

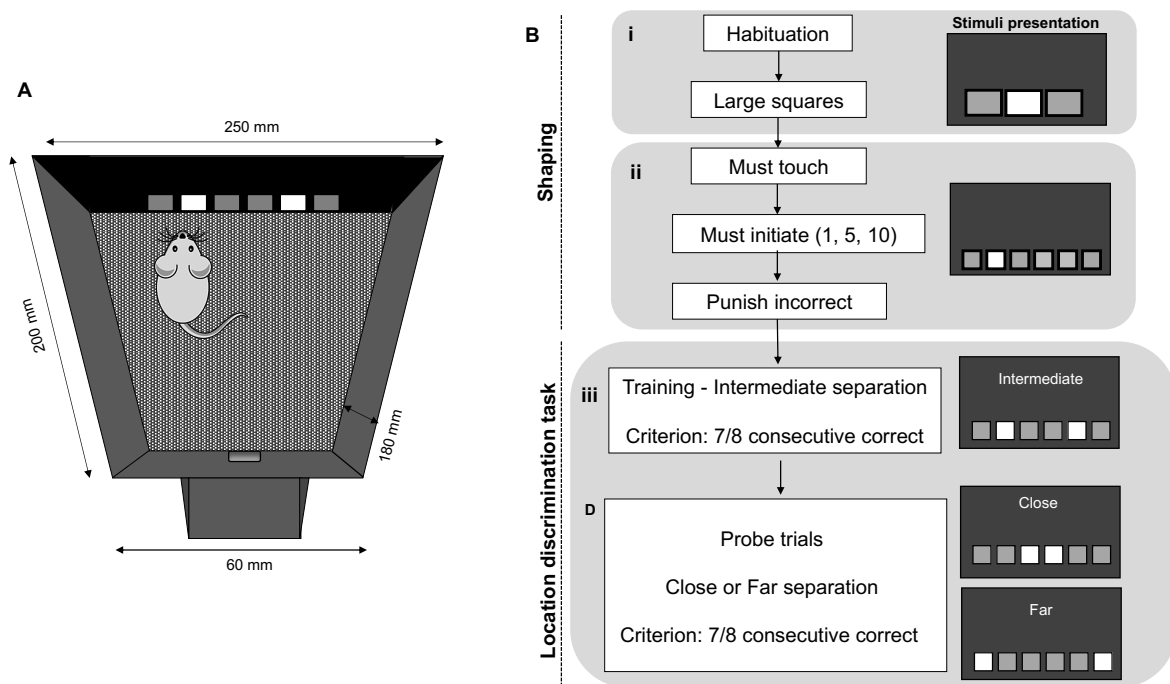
223 **2.7.2 Habituation to condensed milk**

224 To habituate animals to the reward (condensed milk) to be used in the location
225 discrimination task, animals were given the opportunity to consume either condensed
226 milk or water. Preference for condensed milk was calculated as a percentage of total
227 consumption for each of the five days during which water and milk were available.

228 **2.7.3 Location discrimination task**

229 To assess pattern separation, we used an adaptation of the Location Discrimination
230 (LD) task as described in Hvoslef-Eide et al. (2013)⁴⁸ and originally reported by
231 McTighe et al. (2009)⁴⁹. In order to facilitate daily testing of our large behavioural
232 cohort, we implemented shorter, 20 minute test sessions rather than the 60 minute
233 originally reported^{10,12,44,50,51}. Within each session, subjects could complete a
234 maximum of 60 trials. The task was delivered in a touch screen operant chamber
235 (Campden Instruments Ltd., UK; Figure 1A). Animals first went through a period of
236 shaping (Figure 1B,i-ii), which accustomed them to making nose-poke responses to
237 illuminated square stimuli at the front of the chamber, for which they received a reward
238 of condensed milk. Having completed shaping, subjects were moved onto task training
239 on a case-by-case basis to prevent overtraining ⁴⁸.

240



241

242 **Figure 1. Location discrimination (LD) task.** A) Campden Instruments Ltd. mouse
 243 operant touchscreen chamber. The apparatus was housed inside sound-proof, sealed
 244 cubicles. The touchscreen was situated at the front of the chamber and black plastic
 245 masks with apertures were superimposed upon the touchscreen to direct nose pokes
 246 to the appropriate area of the screen on which stimuli were displayed. The mask used
 247 depended on the stage of training (see B). To the rear of the chamber, a magazine
 248 unit was integrated through which measured liquid rewards were delivered. In order to
 249 record the subject's movement, two photo-beams extended between the sidewalls
 250 parallel to the touchscreen and reward delivery area. The chamber floor was a
 251 perforated stainless steel raised above a tray filled with sawdust. B) Task structure.
 252 i) The initial stage of shaping consists of habituation and large squares. This stage
 253 teaches subjects to touch the screen to obtain reward. ii) The latter half of the shaping
 254 stage trains subjects to responds to smaller stimuli, to self-initiate trials and respond
 255 only to the illuminated stimulus. iii) After fulfilling criteria, subjects began training with
 256 stimuli at an intermediate separation After reaching criterion at intermediate separation

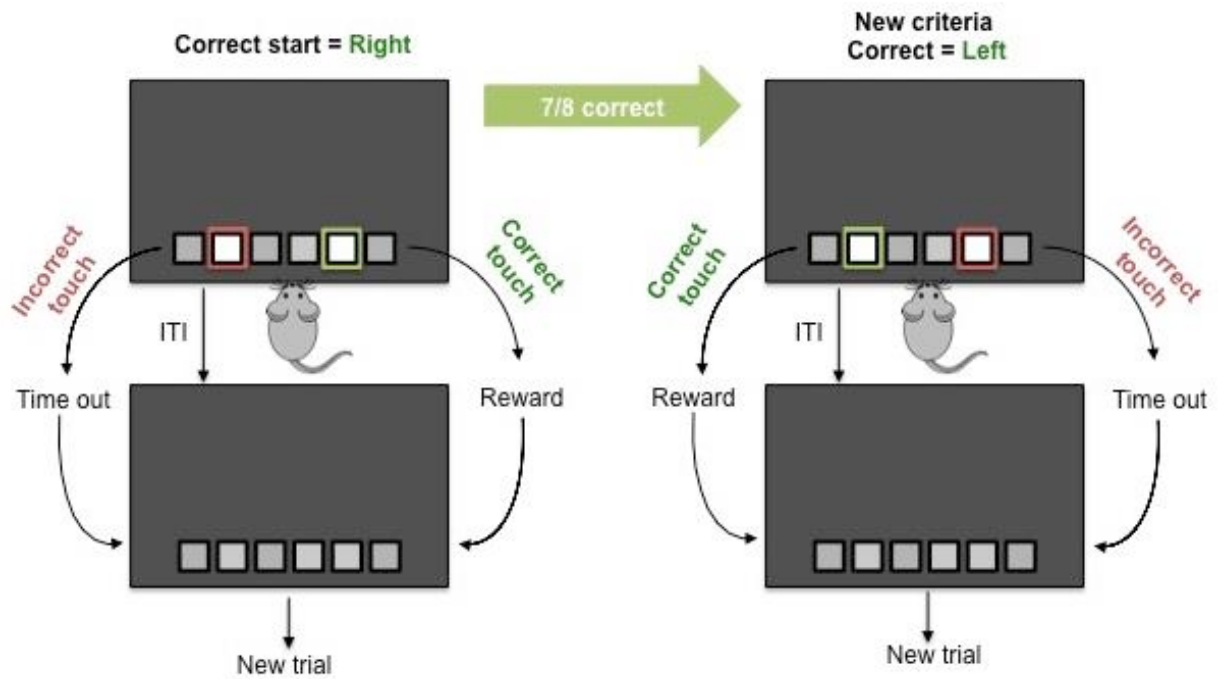
257 training, subjects progress to task probe trials in which stimuli are presented at either
258 close or far separations.

259

260 **2.7.4 Task training**

261 This stage saw the introduction of spatial discriminations, owing to the dual
262 presentation of stimuli on the touchscreen, separated by an intermediate distance
263 (response windows 2 and 5, Figure 1B,iii). One location (e.g., left) was designated as
264 correct, whereas the other illuminated position (e.g., right) was incorrect. Animals were
265 required to complete seven out of eight consecutive trials correct to reach criterion,
266 after which the reward contingencies were reversed so that the previously incorrect
267 location now became correct (Figure 2). Animals then had to achieve seven out of
268 eight correct responses in the new location to attain criterion (reversal). Reward
269 contingencies continued to reverse after each criterion was reached. The reversal
270 element of the task reduces the likelihood that animals develop a side bias or use non-
271 spatial strategies to complete the task^{12,48}. Between consecutive sessions (i.e., on
272 subsequent days of training) the correct stimulus position remained consistent (e.g., if
273 a session ended with the left stimulus being rewarded, the subsequent session, on the
274 next day, would also begin with the left stimulus being rewarded). Subjects were
275 considered to have completed training when they were able to achieve twenty trials or
276 more per session, with a minimum of one reversal (i.e., reaching criterion twice) per
277 session, on each of two consecutive days.

278



279

280 **Figure 2. Trial structure for training stage and probe trials.** Left panel shows a
 281 subject beginning a training session with the right-sided location designated correct. If
 282 an incorrect response is made, stimuli disappear and time-out occurs followed by a 10
 283 second ITI, after which a new trial can be initiated. If a correct response is made,
 284 stimuli disappear, a reward can be collected and a new trial initiated after a 10 second
 285 ITI. If the subject makes 7 correct responses in 8 consecutive trials, the reward
 286 contingency is reversed and the left sided stimulus is now rewarded (right panel). The
 287 same process then ensues until the subject reaches criteria and another reversal
 288 occurs, after which the right side will be rewarded once again.

289

290 **2.7.5 Probe trials**

291 Having met criteria on the training stage, subjects were advanced to a series of probe
 292 sessions (Figure 1B,iii). Trials followed the same structure as the training stage (Figure
 293 2), except for the addition of a spatial discrimination manipulation; sessions featured

294 either far stimulus separations (positions 1 and 6 illuminated) or close stimulus
295 separation (positions 3 and 4 illuminated; Figure 1B,iii). Within one session, all
296 stimulus presentations were either close or far, and each subject received sessions of
297 the same probe type on two consecutive days. The rewarded location did not change
298 between day one and two (unless the subject had finished on a reversal), for example
299 if a subject finished their session on day 1 with the left location being rewarded, they
300 would continue with the left stimulus being rewarded on day 2 until they reached
301 criterion and a reversal occurred. Animals starting on close or far, and with left and
302 right rewarded stimuli, were counterbalanced across groups. Animals received two
303 pairs of probe trials across 4 separate days, with this sequence being repeated twice,
304 meaning that all animals experienced 4 sessions of each separation.

305 **2.7.8 LD task data analysis**

306 For data analysis, all performance metrics including trials to criterion and percentage
307 correct responses to criterion were calculated across all 4 sessions of each separation.
308 In the instance animals did not attain any criteria, which was more common under the
309 close stimuli separation, the number of trials until the completion of probe trials of the
310 same type was substituted to prevent missing data.

311 **2.8 Statistics**

312 All statistical analyses were carried out using GraphPad Prism 8.4.1 (GraphPad
313 Software, CA, USA). Data was assessed for equality of variances using the Brown-
314 Forsythe test and then appropriate parametric (t test, one-way or two-way ANOVA) or
315 non-parametric (Kruskal-Wallis) tests used. The main between-subjects' factor for
316 ANOVA analyses was GENOTYPE (WT, $C3^{-/-}$ or $C3aR^{-/-}$). For morphological analyses,

317 there was an additional within-subjects factor of BLADE (suprapyramidal,
318 infrapyramidal) and for BrdU long-pulse migration analyses there was a within-
319 subjects factor of BIN (1,2,3,4). For the condensed milk habituation experiment, there
320 was a within-subject factors of SESSION (3-7) and for analysis of LD task probe trial
321 data, there was an additional within-subjects factor of SEPARATION (Close, Far). As
322 we predicted differences in the close but not the far condition, planned comparisons
323 using Tukey posthoc tests were carried out to analyse probe trial performance
324 between genotypes. For migration analyses, planned comparisons were used to
325 compare the proportion of BrdU⁺ cells between genotypes at each bin. For all other
326 analyses, posthoc pairwise comparisons were performed using the Tukey or Dunn's
327 tests for parametric or non-parametric analyses, respectively. For all analyses, alpha
328 was set to 0.05 and exact p values were reported unless p<0.0001. All p values were
329 multiplicity adjusted⁵². Data are expressed as mean ± standard error of the mean.

330
331
332
333
334
335
336
337
338
339
340
341
342
343
344
345
346
347
348
349
350
351
352

353 **3. Results**

354

355

356

357 **3.1 Lack of C3/C3aR does not affect progenitor cell proliferation or neuronal**

358 **fate choice**

359 Wildtype, *C3*^{-/-} and *C3aR*^{-/-} mice were injected with thymidine analogue BrdU

360 (100mg/kg, I.P) 6 hours prior to sacrifice, and brain tissue harvested to quantify uptake

361 (Figure 3A). We also co-stained tissue with the endogenous proliferation marker Ki67

362 (Figure 3B). There were no differences in the total number of BrdU⁺ cells in the granule

363 cell layer (GCL; Figure 3C) or the total number of Ki67⁺ cells (Figure 3D), or in the

364 distribution of these cells in dorsal and ventral regions of the hippocampus (Figure

365 S1A). The mitotic index (BrdU⁺Ki67⁺/BrdU⁺) was also unaltered, suggesting no

366 differences in cell cycle speed between genotypes (Figure 3E). Additionally, the area

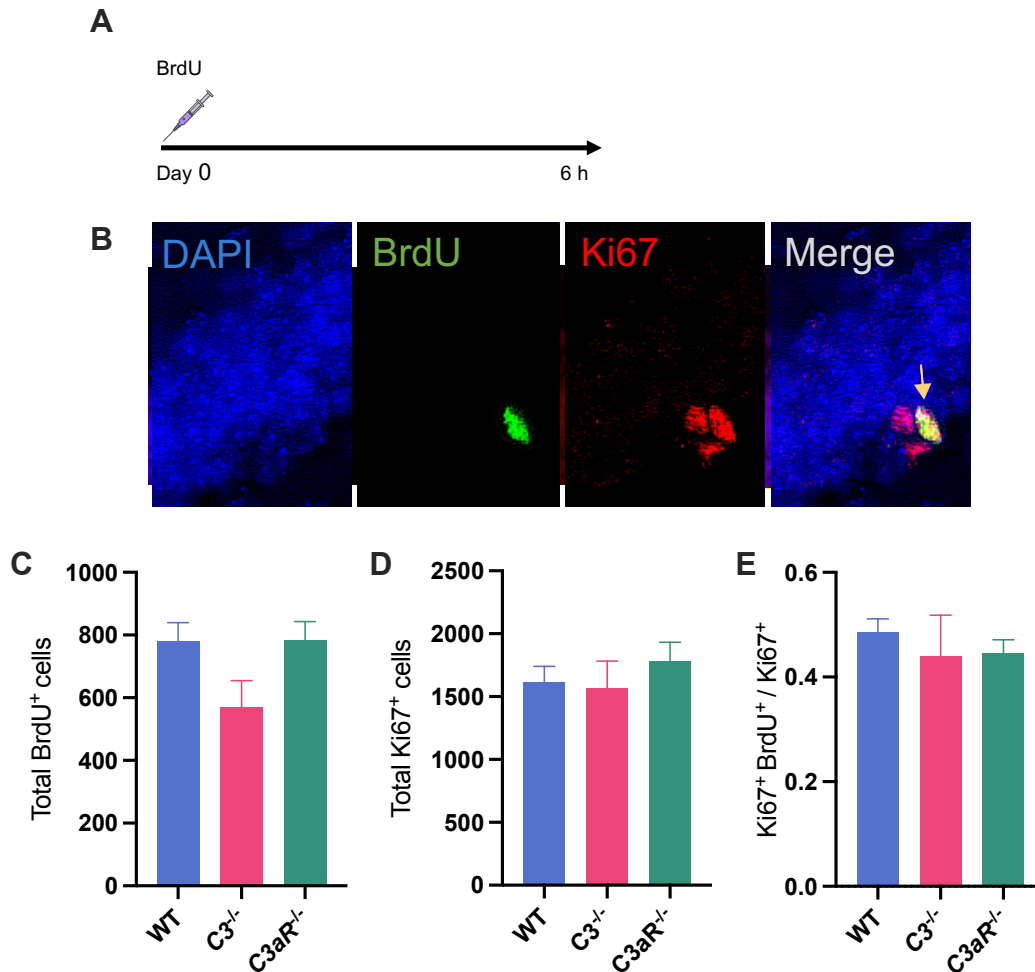
367 of the GCL (measured in both dentate gyri of each section) was equivalent between

368 genotypes (Figure S2A). We also investigated the location of BrdU-labelled cells within

369 the dentate. In the absence of C3 and C3aR, we did not see any differences in the

370 number of ectopically located (either in the hilus or inner molecular layer) BrdU⁺ Ki67⁺

371 cells (Figure S2B).



372

373 **Figure 3. C3/C3aR deficiency does not impact acute proliferation in the dentate**

374 **gyrus. (A)** Animals were injected with BrdU (100mg/kg, I.P) 6 hours prior to sacrifice,

375 and brain tissue harvested to quantify BrdU uptake. **(B)** Immunohistochemistry was

376 performed for BrdU and Ki67 reactivity. Panel contains representative example of

377 BrdU and Ki67 staining in the granule cell layer. Arrow indicates double positive BrdU⁺

378 Ki67⁺ cells situated in the sub granular zone. **(C)** Total number of BrdU⁺ cells WT

379 779.33±60.01, C3^{-/-} 570.00±84.26, C3aR^{-/-} 782.6±60.28; F_{2,13}=0.2.87, p=0.6926. **(D)**

380 Total number of Ki67⁺ cells; WT 1614.66±126.94, C3^{-/-} 1568.58±213.25, C3aR^{-/-}

381 1781.33±151.23; F_{2,15}=0.445, p=0.6491. **(E)** Proportion of BrdU⁺ proliferating (Ki67⁺)

382 cells; WT 0.48±0.02, C3^{-/-} 0.43±0.07, C3aR^{-/-} 0.44±0.02; F_{2,13}=0.390, p=0.6850. Data

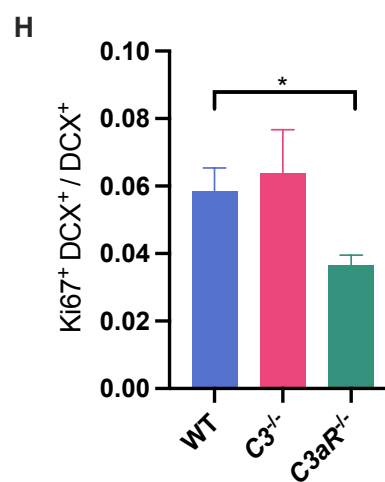
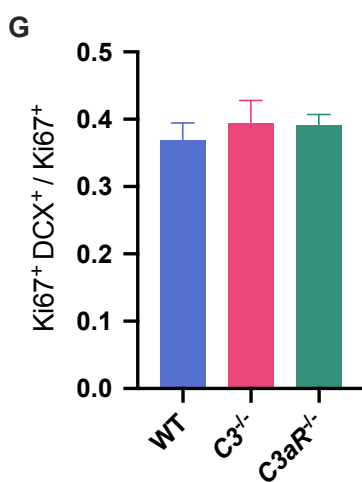
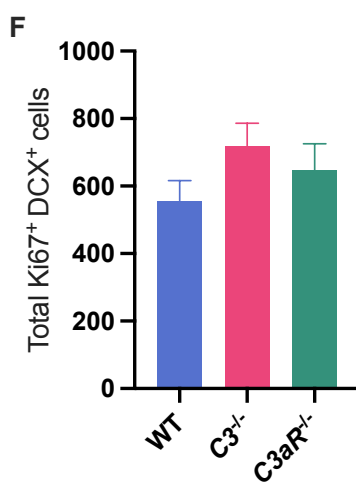
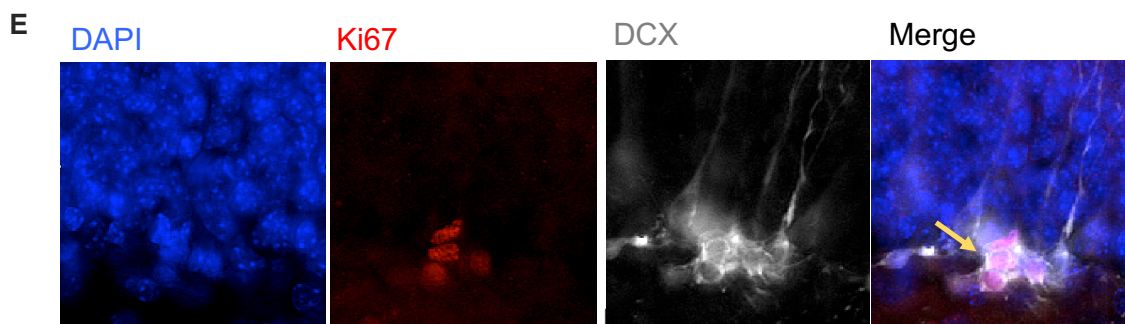
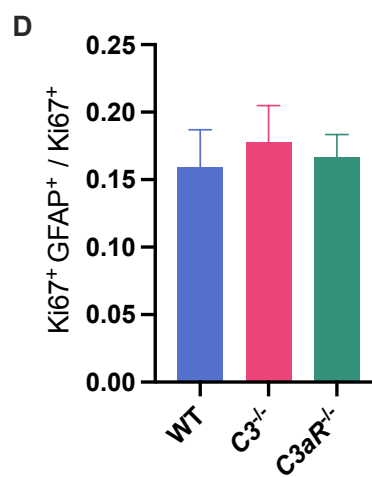
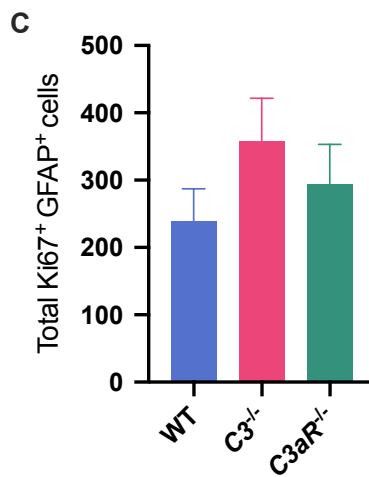
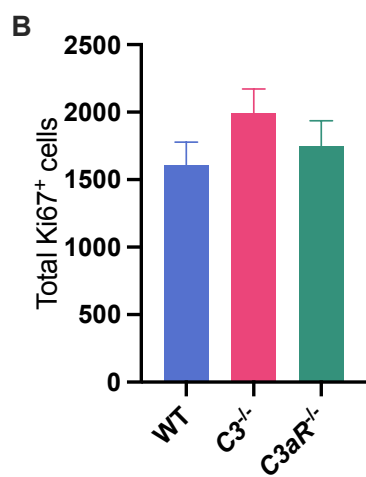
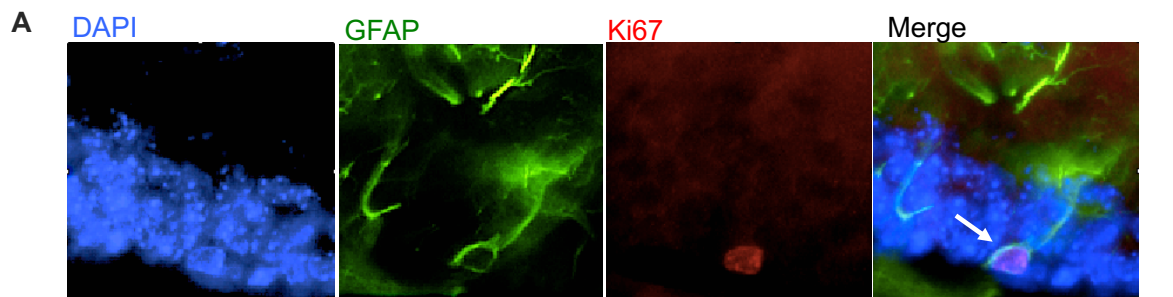
383 are expressed as mean ± S.E.M. Wildtype N =6, C3^{-/-} N =4, C3aR^{-/-} N =6.

384 In a separate cohort of animals, we investigated the phenotype of proliferating cells
385 (Ki67⁺) in the dentate gyrus using the glial marker GFAP and immature neuronal
386 progenitor marker doublecortin (DCX; Figure 4A&E). In this cohort there were again
387 no differences in the total number of Ki67⁺ cells (Figure 4B). There were no differences
388 in the number of proliferating type 1 cells (Ki67⁺GFAP⁺ cells within the GCL with apical
389 morphology; Figure 4C) and these cells accounted for a similar proportion of the total
390 Ki67⁺ population between genotypes suggesting no differences in the proliferative
391 stem cell pool (Figure 4D). The total number of proliferating type 2b/3 neuronal
392 progenitor cells was also unchanged (Ki67⁺DCX⁺; Figure 4F) and these cells again
393 accounted for a comparable proportion of the proliferative population across
394 genotypes (Figure 4G) indicating that early neuronal fate choice was unaffected by
395 absence of C3/C3aR.

396

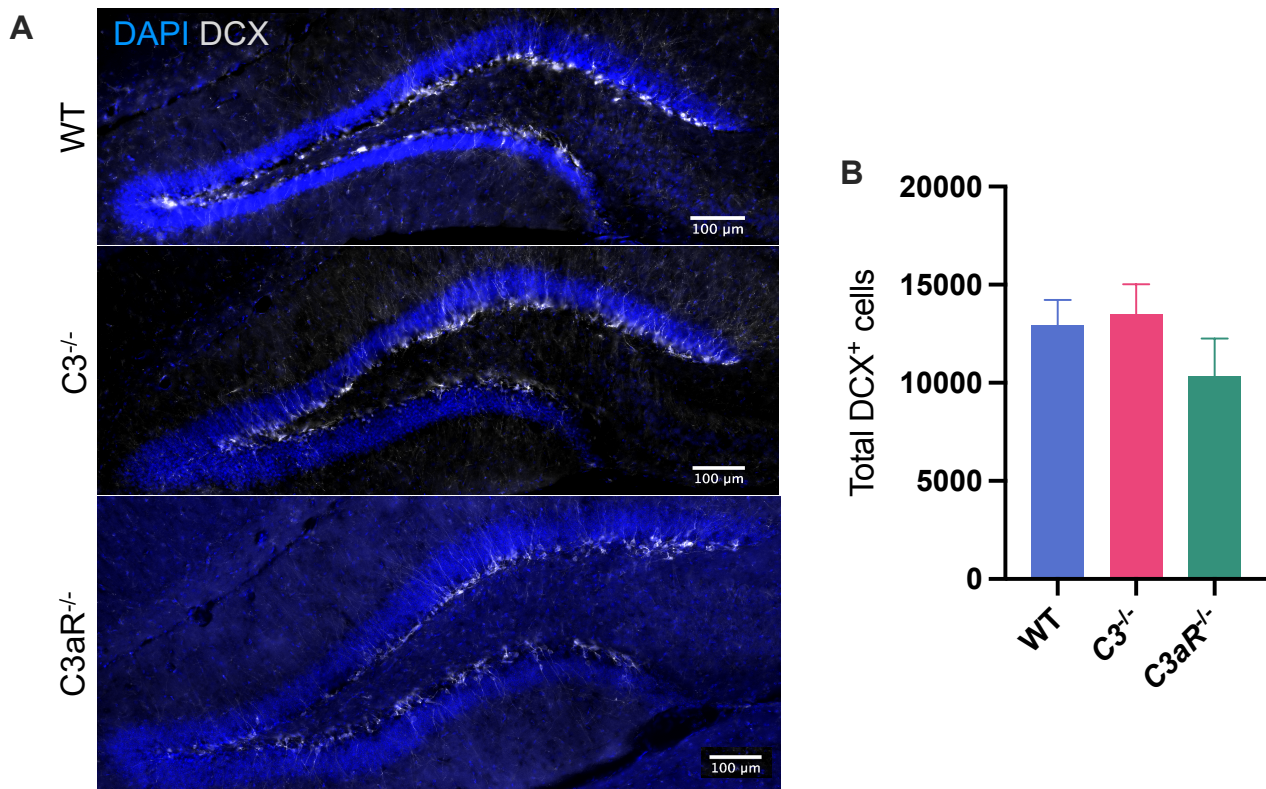
397 Of the total neuronal progenitor (DCX⁺) population, significantly fewer of these were
398 in the cell cycle in *C3aR*^{-/-} mice compared to wildtype (p=0.0386), whereas *C3*^{-/-} mice
399 were unchanged (Figure 4H). Despite a trend towards slight decrease in the total
400 number of DCX⁺ cells in *C3aR*^{-/-} mice (Figure 5A&B) this was not significantly different
401 to WT or *C3*^{-/-} mice. Taken together, these findings indicate that the decreased growth
402 fraction of neural progenitor cells in *C3aR*^{-/-} mice did not affect the overall production
403 of neural progenitors. There were no genotype differences in the distribution of any of
404 the aforementioned cell types along the hippocampal longitudinal axis (Figure S1 B-
405 D).

406



408 **Figure 4. C3/C3aR deficiency does not impact the proliferation of type 1 radial**
409 **glial cells whereas C3aR specifically reduces the proportion of neuroblasts that**
410 **are proliferating.** In a further cohort of animals, immunohistochemistry was
411 performed for Ki67, GFAP and doublecortin (DCX) reactivity. **(A)** Representative
412 example of Ki67 and GFAP staining. Ki67⁺ GFAP⁺ cells were only counted if they
413 demonstrated the apical morphology characteristics of type 1 radial glial cells and were
414 situated in the granule cell layer (as indicated by white arrow). **(B)** Total number of
415 Ki67⁺ cells. WT 1606.00±172.00, C3^{-/-} 1993.00±178.6, C3aR^{-/-} 1749.00±188.7;
416 F_{2,15}=1.19, p=0.3321. **(C)** Total number of proliferating type 1 radial glial cells (Ki67⁺
417 GFAP⁺); WT 238.50±48.80, C3^{-/-} 357.90±63.91, C3aR^{-/-} 292.80±60.30, F_{2,15}=1.06,
418 p=0.3703. **(D)** Proportion of Ki67⁺ GFAP⁺ cells in total Ki67⁺ population; WT 0.15±0.02,
419 C3^{-/-} 0.17±0.02, C3aR^{-/-} 0.16±0.01; F_{2,15}=0.143, p=0.8678. **(E)** Representative
420 example of Ki67 and DCX staining. Yellow arrow indicates a cluster of double positive
421 cells. **(F)** Total number of immature neuronal progenitor cells in the cell cycle (Ki67⁺
422 DCX⁺). WT 557.10±58.87, C3^{-/-} 719.00±67.24, C3aR^{-/-} 647.60±77.54; F_{2,15}=1.41,
423 p=0.2744. **(G)** Proportion of Ki67⁺ DCX⁺ cells in total Ki67⁺ population. WT 0.37±0.02,
424 C3^{-/-} 0.39±0.03, C3aR^{-/-} 0.39±0.01; F_{2,15}=0.278, p=0.7614. **(H)** Proportion of Ki67⁺
425 DCX⁺ cells in total DCX⁺ population. WT 0.05±0.006, C3^{-/-} 0.06±0.01, C3aR^{-/-}
426 0.03±0.007; H₂=7.45, p=0.0172. Data are mean ± S.E.M. Wildtype N =6, C3^{-/-} N =6,
427 C3aR^{-/-} N =6. * = p≤0.05 for *post-hoc* genotype comparisons.

428



429
 430 **Figure 5. The total number of immature neuronal progenitor cells is unaffected**
 431 **by lack of C3 and C3aR. (A)** Representative example of DCX staining in different
 432 genotypes. **(B)** Total number of DCX⁺ cells. WT 12904±1323, C3^{-/-} 13502±1530, C3aR^{-/}
 433 ^{-/} 10344±1912; $F_{2,14}=1.08$, $p=0.3678$. Data are mean ± S.E.M. Wildtype $N = 6$, C3^{-/-} N
 434 $= 5$, C3aR^{-/} $N = 6$.

435

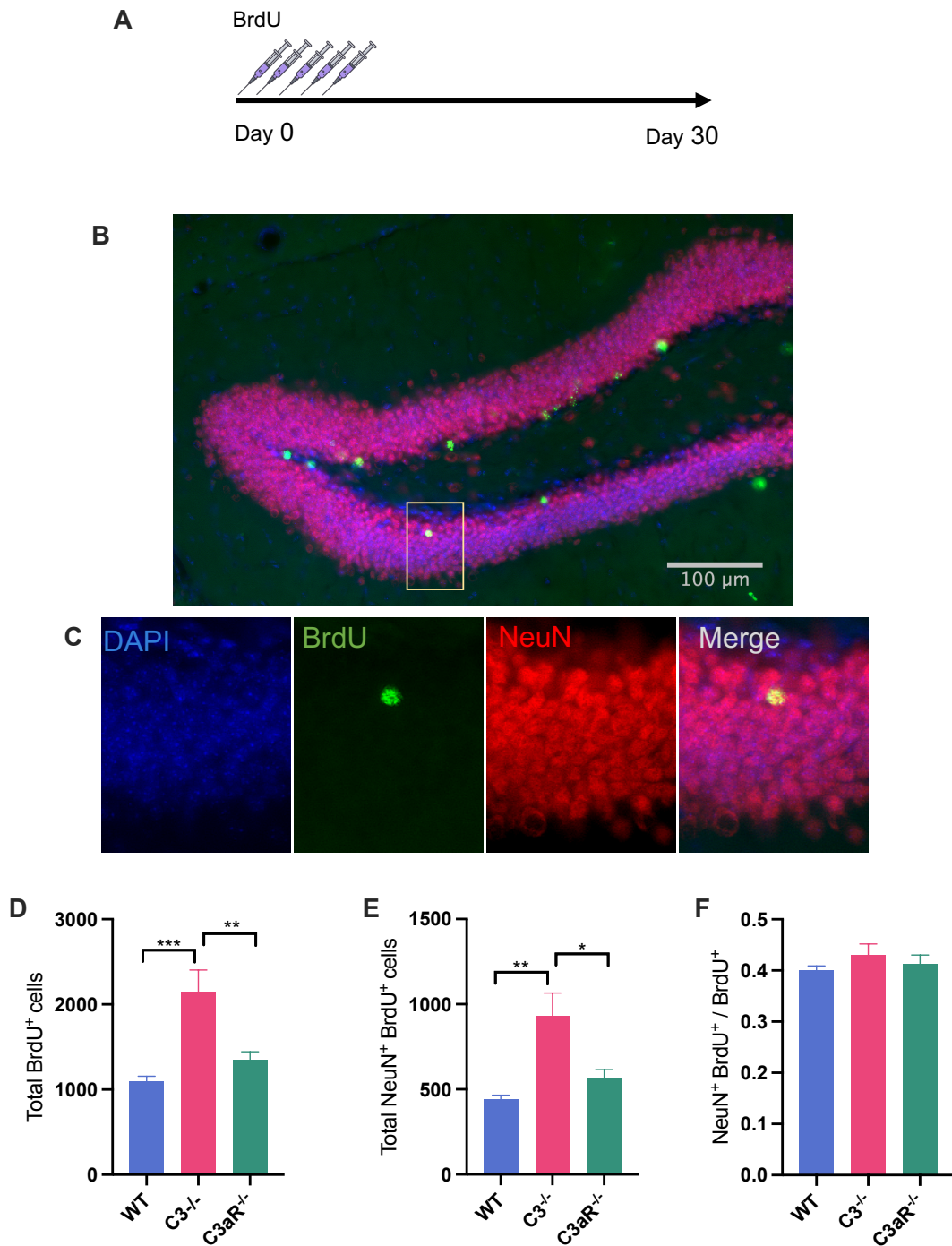
436 **3.2 Lack of C3 results in increased neurogenesis due to greater survival of** 437 **newborn neurons**

438 In order to track the maturation and survival of new neurons born in the dentate gyrus,
 439 mice were injected with BrdU (100mg/kg, i.p) daily for 5 days and sacrificed 30 days
 440 later (Figure 6A). Tissue was processed for BrdU and NeuN immunoreactivity to detect
 441 surviving adult-born neurons (Figure 6B&C). We observed a significantly greater
 442 number of BrdU⁺ cells throughout the hippocampus (Figure S1 E) in C3^{-/-} mice
 443 compared to both wildtype ($p=0.0007$) and C3aR^{-/} mice ($p=0.0051$; Figure 6D). There

444 were also a greater total number of cells double positive for BrdU and NeuN (Figure
445 6E) in $C3^{-/-}$ mice compared to both wildtype ($p=0.0022$) and $C3aR^{-/-}$ mice ($p=0.0139$;
446 Figure 6E). The proportion of BrdU labelled cells adopting neuronal fate ($\text{BrdU}^+ \text{NeuN}^+$)
447 was unaltered between genotypes (Figure 6F).

448

449 Given that the total number of proliferating cells (Figure 3), the number of proliferating
450 cells that were expressing DCX (Figure 4F&G) and the proliferation dynamics of
451 immature neurons (Figure 4H) were all unchanged in $C3^{-/-}$ mice, we were confident
452 that there were no changes in early neuronal differentiation or proliferation and
453 therefore the net increase we observed of $\text{NeuN}^+ \text{BrdU}^+$ cells in $C3^{-/-}$ mice (Figure 6)
454 suggested a specific effect of C3 on the survival of adult born GCs.



455

456 **Figure 6. C3 influences the number of surviving adult-born neurons but does**

457 **not affect fate choice.** (A) Animals were injected with BrdU (100mg/kg, I.P) once

458 daily for 5 days and sacrificed 30 days later. (B) Brain tissue was sectioned at 40μm

459 and processed for BrdU and NeuN immunoreactivity. Micrograph shows

460 representative staining. Yellow bow indicates example of BrdU⁺ NeuN⁺ cell magnified

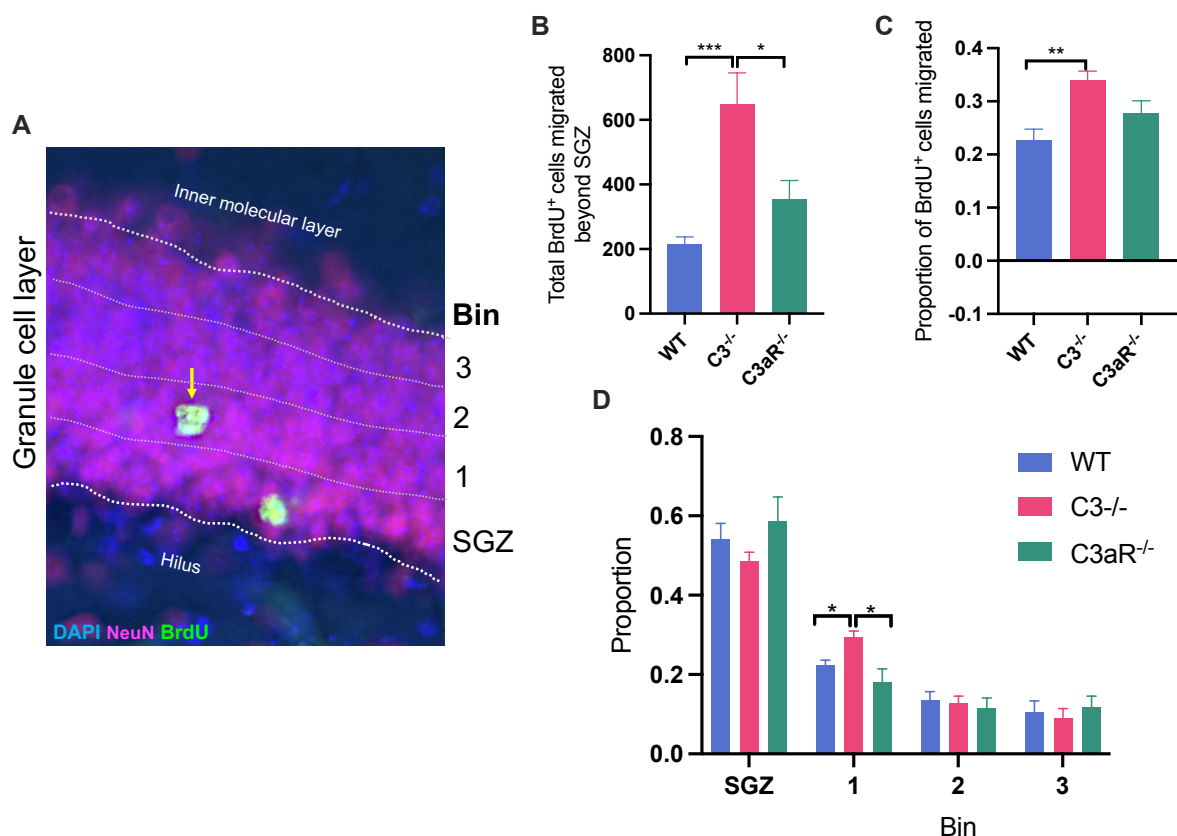
461 in. **(C)** Representative example of BrdU⁺ NeuN⁺ double positive cell. **(D)** Total number
462 of BrdU⁺ cells. WT 1096±60.9, C3^{-/-} 2152±253, C3aR^{-/-} 1344±100, F_{2,16}=12.0,
463 p=0.0006. **(E)** Total number of BrdU⁺ NeuN⁺ cells. WT 439±26.0, C3^{-/-} 932±134, C3aR^{-/-}
464 559±56.5; F_{2,16}=9.25, p=0.0021. **(F)** Proportion of total BrdU⁺ cell population double
465 positive for NeuN⁺ (neuronal fate). F_{2,16}=0.792, p=0.4700. Data are mean ± S.E.M.
466 Wildtype N =6, C3^{-/-} N =6, C3aR^{-/-} N =7. *, ** and *** represent p≤0.05, p≤0.01 and
467 p≤0.001 for *post-hoc* genotype comparisons, respectively.

468

469 **3.3 Lack of C3 results in accelerated migration of surviving new neurons outside** 470 **the sub granular neurogenic niche**

471 As adult-born neurons mature, they migrate from the sub granular zone (SGZ) deeper
472 into the granule cell layer (GCL)⁵³ as they extend their apical dendrites further into the
473 molecular layer⁵⁴. To measure the migration of surviving neurons labelled in the 30-
474 day BrdU pulse-chase experiment, we measured the distribution of BrdU⁺ cells within
475 the GCL. We divided the GCL into four equal bins, the innermost of which
476 corresponded to the SGZ, the band approximately two cell bodies thick that follows
477 the GCL-hilar border. The subsequent two bins (1 & 2) represented the middle layers
478 of the GCL, whereas bin 3 consisted of the outermost portion of the GCL proximal to
479 the inner molecular layer (Figure 7A). There were no significant differences in the
480 thickness of the GCL between wildtype and C3^{-/-} mice (p=0.2622) although C3aR^{-/-}
481 mice did have a thicker GCL than wildtypes (p=0.0407; Figure S3) by approximately
482 ~3 μm, less than one cell width. We analysed the number of BrdU⁺ cells that had
483 migrated beyond the SGZ (i.e., occupied bins 1-3) and found that significantly more
484 BrdU⁺ cells had migrated in C3^{-/-} mice compared to wildtype mice (p=0.0009) and
485 C3aR^{-/-} mice (p=0.0146; Figure 7B). The proportion of BrdU⁺ cells that had migrated

486 was also significantly increased in $C3^{-/-}$ mice compared to wildtype ($p=0.0055$) but not
 487 compared to $C3aR^{-/-}$ mice ($p=0.1367$; Figure 7C), suggesting that the increased
 488 numbers of migrated cells in $C3^{-/-}$ mice were not merely due to surplus cells migrating
 489 normally, but instead due to altered migratory patterns of newborn neurons. Since we
 490 anticipated differences in the proportion of cells that migrated in $C3^{-/-}$ mice, we
 491 conducted planned comparisons of BrdU⁺ cells within the SGZ or bins 1-3. In $C3^{-/-}$
 492 mice, we found an exaggerated proportion of cells in bin 1 compared to wildtype
 493 ($p=0.0119$) and $C3aR^{-/-}$ mice ($p=0.0312$) suggesting accelerated migration of surviving
 494 immature GC neurons in the absence of C3.
 495



496
 497 **Figure 7. Lack of C3 alters the migration of adult born neurons into the granule**
 498 **cell layer. (A)** Example of how we divided the GCL into four equal portions or bins.
 499 The inner-most bin, proximal to the hilus, comprised the sub granular zone (SGZ).

500 Bin 1 and 2 represented the middle of the GCL, whereas bin 4 represented the
501 outermost layer of the GCL proximal to the inner molecular layer. **(B)** Total number of
502 BrdU⁺ cells that had migrated beyond the SGZ (i.e., in bin 1-3). Wildtype 271±20.8,
503 C3^{-/-} 648±97.2, C3aR^{-/-} 356±56.9, F_{2,16}=10.8, p=0.0011. **(C)** Migrated cells (BrdU⁺ cells
504 found beyond the SGZ) as a proportion of total GCL BrdU⁺ cells. Wildtype 0.22±0.02,
505 C3^{-/-} 0.34±0.01, C3aR^{-/-} 0.27±0.02, F_{2,16}=7.18, p=0.0059. **(D)** BrdU⁺ cells found in each
506 bin as a proportion of total GCL BrdU⁺ cells. Main effect of BIN; F_{1,72, 27.5}=88.1,
507 p<0.0001; GENOTYPE F_{2,16}=0.139, p=0.8711; BIN × GENOTYPE F_{6,48}=1.51,
508 p=0.1936. Data are mean ± S.E.M. A total of 576 BrdU⁺ cells were analysed from N=6
509 wildtype animals, 1139 BrdU⁺ cells from N=6 C3^{-/-} animals and 869 BrdU⁺ cells from
510 N=7 C3aR^{-/-} animals. *, ** and *** represent p≤0.05, p≤0.01 and p≤0.001 for *post-hoc*
511 genotype comparisons, respectively.

512

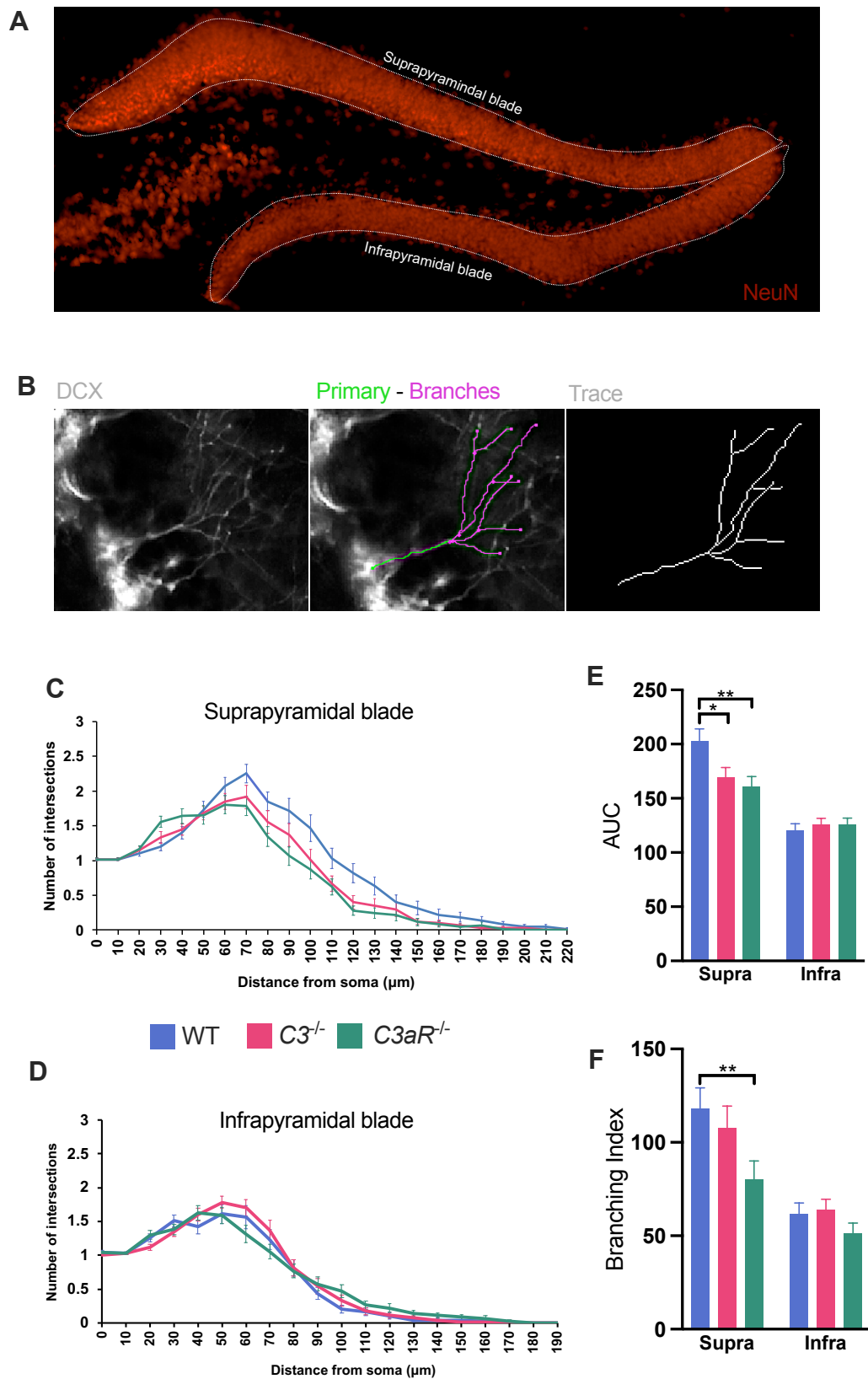
513

514 **3.4 Lack of C3/C3aR reduces morphological complexity of immature neuronal** 515 **progenitor cells**

516 We next used Sholl analysis to investigate the morphology of immature DCX⁺ neurons
517 with vertically oriented apical processes in the GCL. These cells are typically type 3
518 cells², the stage at which the greatest morphological changes occur⁵³. Due to the
519 known differences in the dendritic trees of immature neurons located in the
520 suprapyramidal blade versus the infrapyramidal blade of the dentate⁵⁵, we analysed
521 cells from each blade separately (Figure 8A). Cells were systematically randomly
522 sampled, and their dendritic trees manually traced and subjected to Sholl analysis
523 (Figure 8B). The resulting Sholl profiles indicated differences in both knockouts in the

524 suprapyramidal blade beyond ~70 μm from the cell soma (Figure 8C) but not the
525 infrapyramidal blade (Figure 8D). This was confirmed by analysis of area under the
526 curve, which revealed that both $C3^{-/-}$ and $C3aR^{-/-}$ DCX⁺ cells had a reduced AUC in
527 the suprapyramidal, but not the infrapyramidal blade, compared to wildtypes (Figure
528 8E).

529 At the outset, these differences could reflect both neurite length and branching⁴⁷ and
530 we therefore employed further measures to differentiate these possibilities. The
531 branching index⁴⁷ (BI; a specific measure of neurite ramification) of $C3aR^{-/-}$ DCX⁺ cells
532 was reduced in the suprapyramidal blade compared to that of wildtype and $C3^{-/-}$
533 (Figure 8F) suggesting less complex dendritic branching. In addition, there was a trend
534 towards reduced primary path length of suprapyramidal DCX⁺ cells in $C3aR^{-/-}$ cells
535 compared to wildtype (Figure S4 A). A similar trend was observed in average branch
536 length (Figure S4 B) and $C3aR^{-/-}$ DCX⁺ cells had significantly fewer branches
537 compared to wildtype and $C3^{-/-}$ cells, regardless of blade (Figure S4 C). These results
538 indicated an overall reduced dendritic complexity in the absence of C3aR, reflected by
539 decreased branch length, number and ramification in $C3aR^{-/-}$ DCX⁺ cells.



540

541 **Figure 8. Absence of C3/C3aR influences the morphology of immature neurons.**

542 **(A)** Location of suprapyramidal (most dorsal) and infrapyramidal (most ventral) blades.

543 **(B)** Left panel shows a representative example of a DCX⁺ immature neuron selected
544 at random for Sholl analysis. Middle panel shows the tracing in progress, with primary
545 process in green and branches in magenta. Right panel depicts the resulting trace,
546 upon which Sholl analyses are based. **(C)** Sholl curve for cells in suprapyramidal blade
547 **(D)** Sholl curve for cells in infrapyramidal blade. **(E)** Area under the curve (AUC)
548 analysis. WT 202.41±11.74, C3^{-/-} 169.41±8.97, C3aR^{-/-} 160.91±9.25. BLADE ×
549 GENOTYPE interaction F_{2,386}=4.68, p=0.0098 [WT vs. C3^{-/-} p=0.0167, WT vs. C3aR^{-/-}
550 ^{-/-} p=0.0017, C3^{-/-} vs. C3aR^{-/-} p=0.7573] and main effect of BLADE; F_{1,386}=65.9,
551 p=<0.0001. **(F)** Branching Index (BI); WT 117.39± 10.88, C3^{-/-} 107.39±11.35, C3aR^{-/-}
552 79.98±9.79; main effect of GENOTYPE F_{2,272}=4.29, p=0.0147 *post hoc* WT vs. C3aR^{-/-}
553 ^{-/-} p=0.0076, C3^{-/-} vs. C3aR^{-/-} p=0.0556, WT vs. C3^{-/-} p=0.7494. Data are mean ± S.E.M.
554 Analyses were of 131 cells from N =6 wildtype animals, 127 cells from N =5 C3^{-/-}
555 animals, and 131 cells from N =6 C3aR^{-/-} animals. * and ** represent p≤0.05 and
556 p≤0.01 respectively for *post-hoc* genotype comparisons.

557

558 Overall, our histological data indicated that lack of C3 specifically increased the
559 survival of adult born neurons and accelerated their migration. Lack of either C3 or
560 C3aR had effects on the morphological development of adult born neurons, though
561 this was more pronounced in the absence of C3aR. We next assessed the functional
562 relevance of these phenotypes for pattern separation, the computational process
563 thought to supported by adult born neurons that is important for distinguishing between
564 similarly encoded spatial or contextual stimuli⁸.

565

566

567 **3.5 *C3aR*^{-/-} mice demonstrate improved pattern separation whereas *C3*^{-/-} show**
568 **evidence of impaired cognitive flexibility**

569 We investigated AHN-related behaviours in a reward-based visual discrimination task
570 using a paradigm previously shown to be sensitive to manipulations of AHN in
571 assaying pattern separation^{44,50,56}. The task required discrimination of stimuli with
572 varying degrees of spatial proximity with closer stimuli placing a greater demand upon
573 pattern separation^{10,12,44}. Mice were initially trained to discriminate the correct
574 response location between two white square stimuli (located in two of six possible
575 locations; Fig 9A) at an intermediate level of spatial separation to a baseline
576 performance criterion of 7 correct responses out of 8. Task difficulty was manipulated
577 from this baseline by introducing probe trials where the stimuli were either further apart
578 (reducing pattern separation requirements) or closer together (increasing pattern
579 separation requirements) than the baseline discrimination (see Fig 9A, probe trials).
580 Prior to beginning training in the touch-screen apparatus, we established equivalent
581 locomotor activity between genotypes (Figure S5A), adapted mice to a water
582 deprivation schedule to motivate reward-orientated behaviour (Figure S5B) and
583 established equal preferences for condensed milk, the liquid foodstuff to be used as
584 reward in the discrimination task (Figure S5C).

585

586 An initial finding was that in the earliest stages of behavioural shaping (Figure S6) and
587 training to baseline criterion (Figure 9B), *C3*^{-/-} mice displayed a relative enhanced
588 performance, requiring fewer trials to reach criterion. Upon reaching baseline
589 performance each animal was subjected to the probe trials. As predicted, task difficulty
590 was increased in the close stimuli separation condition, an effect seen across
591 genotypes as evidenced by an overall reduced percentage of correct responses made

592 in reaching the criterion of 7/8 correct responses (Figure 9D), fewer mean criteria
593 achieved (where the mice could continue responding beyond reaching the first
594 criterion following a reversal of the rewarded stimuli position; Figure 9E) and increased
595 latencies for both correct and incorrect responses (Figure 9H).

596

597 As we anticipated differences in the effects of the close and far probes, we carried
598 out planned comparisons using *posthoc* Tukey tests that revealed an enhanced
599 performance of *C3aR*^{-/-} mice in reaching the first criterion on close probe trials
600 compared to wildtype and *C3*^{-/-} mice. *C3aR*^{-/-} mice were relatively unperturbed by the
601 close separation probe, and under that condition required fewer trials to reach the first
602 criterion compared to both wildtype and *C3*^{-/-} mice (Figure 9C; WT vs *C3aR*^{-/-}
603 $p=0.0150$, *C3*^{-/-} vs. *C3aR*^{-/-} $p=0.0004$). *C3aR*^{-/-} mice also made a greater percentage
604 of correct responses in achieving the first criterion in the close separation probe
605 compared to wildtypes (Figure 9D; WT vs *C3aR*^{-/-} $p=0.0235$, *C3*^{-/-} vs. *C3aR*^{-/-}
606 $p=0.2673$). Although there was a trend towards *C3*^{-/-} mice requiring more trials to reach
607 criterion, their performance was not significantly different to wildtype mice on either
608 the number of trials to first criterion (WT vs. *C3*^{-/-} $p=0.3267$; Figure 9C) or the
609 percentage of correct responses before achieving first criterion (WT vs. *C3*^{-/-} $p=0.5790$;
610 Figure 9D). There were no significant differences between genotypes in the far
611 separation condition in either trials to first criterion or percentage correct responses to
612 first criterion (Figure 9C,D).

613

614 After animals reached the first criterion in either the close or far condition, the spatial
615 position of the rewarded stimulus was reversed and relearning of the contingency was
616 required to reach subsequent criteria. In reality animals rarely reached criterion within

617 the same session especially under the close condition, so we took account of all probe
618 trial sessions of each separation type to calculate the mean number of criteria
619 achieved. Mirroring to an extent the enhanced performance of $C3^{-/-}$ mice at the
620 baseline training stage (Figure 9B), where stimuli were separated by an intermediate
621 distance, $C3^{-/-}$ mice achieved significantly more criteria across sessions than wildtype
622 and $C3aR^{-/-}$ mice under the far separation (Figure 9E; $C3^{-/-}$ vs. WT $p=0.0001$, vs. $C3aR^{-/-}$
623 $p=0.0019$,) but not however at the close separation ($C3^{-/-}$ vs WT $p=0.3077$; vs. $C3aR^{-/-}$
624 $p=0.6302$). This was an important distinction since it implied that the apparent
625 enhanced performance in the far separation condition was not due to an effect on
626 pattern separation, since any advantage would be manifest in the close but not far
627 separation condition.

628

629 We observed that the behaviour of the $C3^{-/-}$ mice was characterised by a general
630 increase in responding resulting in a significantly greater number of trials across all
631 sessions regardless of stimulus separation (Figure 9F). We also noted that $C3^{-/-}$ mice
632 showed a different response style compared to wildtype and $C3aR^{-/-}$ mice,
633 demonstrating decreased response latencies, regardless of accuracy or stimulus
634 separation, although these differences were particularly pronounced at close
635 separations due to the slowing of responses in wildtype and $C3aR^{-/-}$ mice (Fig 9H;
636 correct responses at close $C3^{-/-}$ vs. WT $p=0.1126$; vs. $C3aR^{-/-}$ $p=0.0295$; and incorrect
637 responses at close $C3^{-/-}$ vs. WT $p=0.0011$ vs. $C3aR^{-/-}$ $p=0.0133$). In addition, $C3^{-/-}$ mice
638 made a greater number of inter-trial interval touches across conditions (Figure 9I;
639 Close; $C3^{-/-}$ vs. WT $p=0.0073$; vs. $C3aR^{-/-}$ $p=0.0025$; Far $C3^{-/-}$ vs. WT $p=0.0039$, vs.
640 $C3aR^{-/-}$ $p=0.0150$).

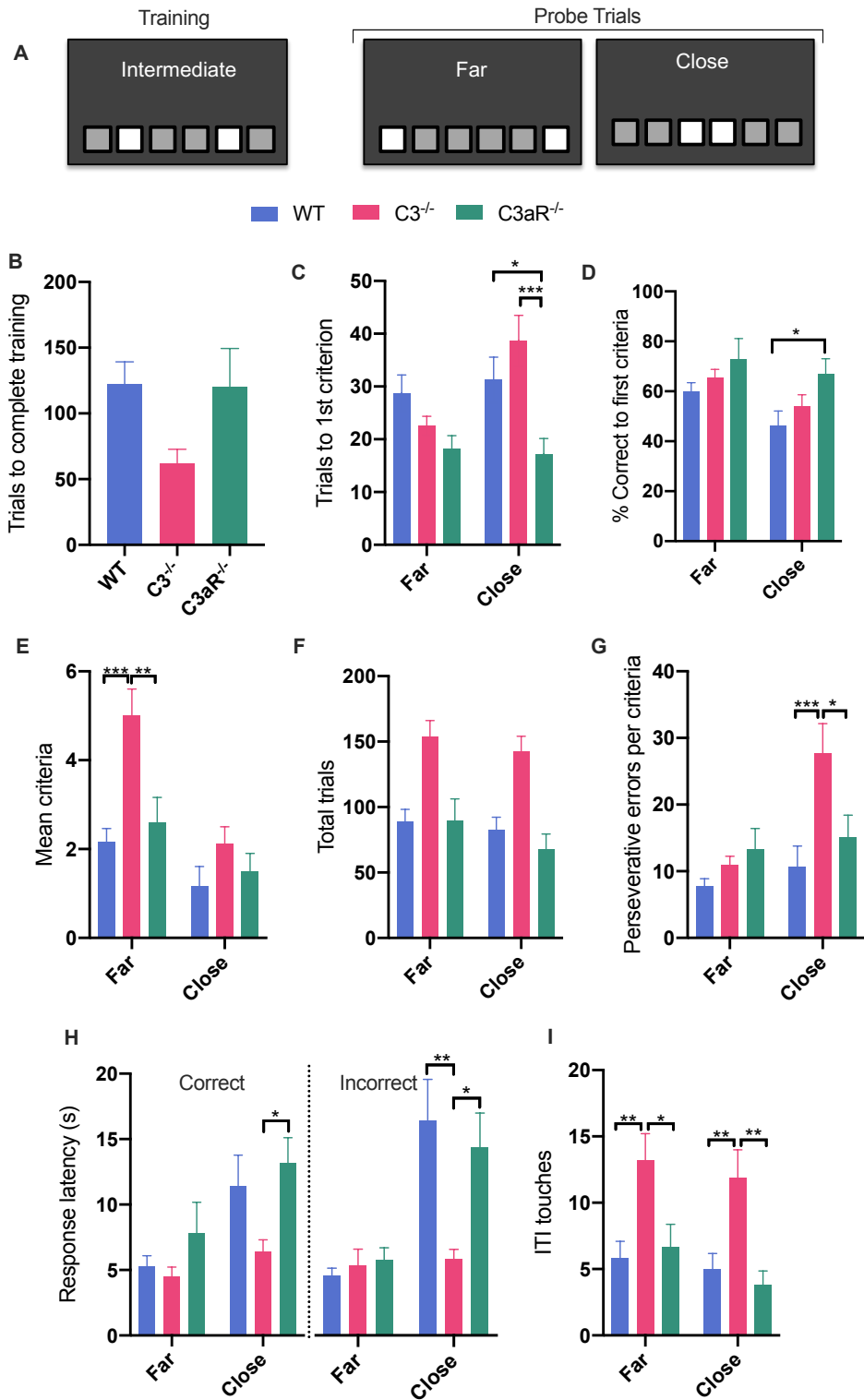
641

642 The pattern of behaviour in the $C3^{-/-}$ mice was reminiscent of impaired behavioural
643 inhibition, that is, a relative inability to suppress inappropriate responding. To test this
644 further we took advantage of the reversal manipulation component of the paradigm
645 and analysed the number of incorrect responses made post-reversal as an index of
646 perseverative responding having first adjusted this for the number of criteria achieved
647 per subject. We found that $C3^{-/-}$ mice made significantly more perseverative errors per
648 criteria when stimuli were close together (Figure 9G; $C3^{-/-}$ vs. WT $p=0.0008$, vs. $C3aR^{-/-}$
649 $p=0.0142$) but not far apart ($C3^{-/-}$ vs. WT $p=0.6512$, vs. $C3aR^{-/-}$ $p=0.8060$). These
650 data were consistent with a deficit in behavioural inhibition manifest under conditions
651 of increased task difficulty where there were increased demands on pattern
652 separation.

653

654 In summary, $C3aR^{-/-}$ showed enhancements in pattern separation abilities, evidenced
655 by improved discrimination performance under conditions where stimuli were highly
656 spatially similar. In contrast, $C3^{-/-}$ behaviour was consistent with deficits in cognitive
657 flexibility arising from impaired behavioural inhibition that were especially marked
658 under conditions of increased task difficulty.

659



660

661 **Figure 9. Performance on the location discrimination task.** (A) Subjects were first
 662 trained on stimuli separated by an intermediate distance, before moving onto probe
 663 trials in which the spatial separation between stimuli was manipulated to tax pattern
 664 separation. Criteria was reached when subjects made 7 out of 8 correct responses on

665 consecutive trials, after which the reward contingency was reversed, and subjects
666 were required to re-learn the contingency to achieve a subsequent criterion. **(B)** Mean
667 number of trials needed to complete training. $H_2=5.59$, $p=0.0610$. **(C)** Trials to first
668 criterion. Planned comparison of genotypes at close; WT 31.08 ± 4.31 vs $C3aR^{-/-}$
669 17.00 ± 2.93 $p=0.0150$, $C3^{-/-}$ 38.33 ± 4.87 vs. $C3aR^{-/-}$ $p=0.0004$, WT vs. $C3^{-/-}$ $p=0.3084$
670 and far; WT 28.50 ± 3.43 vs $C3aR^{-/-}$ 17.90 ± 2.47 $p=0.0851$, $C3^{-/-}$ 22.17 ± 1.82 vs. $C3aR^{-/-}$
671 $p=0.6957$, WT vs. $C3^{-/-}$ $p=0.4238$. **(D)** Percentage of correct responses made in the
672 run up to first criterion; main effect of SEPARATION $F_{(1,28)}=4.64$, $p=0.0400$. Planned
673 comparisons of genotypes at close: WT 46.16 ± 5.98 vs $C3aR^{-/-}$ 67.03 ± 6.05 $p=0.0235$,
674 $C3^{-/-}$ 54.08 ± 4.55 vs. $C3aR^{-/-}$ $p=0.2673$ and far; WT 60.04 ± 3.44 vs $C3aR^{-/-}$ 72.86 ± 8.29
675 $p=0.7731$, $C3^{-/-}$ 65.46 ± 3.34 vs. $C3aR^{-/-}$ $p=0.6440$, WT vs. $C3^{-/-}$ $p=0.7731$. **(E)** Mean
676 criteria achieved across sessions; main effect of SEPARATION $F_{(1,28)}=49.5$, $p<0.0001$.
677 Planned comparisons at close; $C3^{-/-}$ 1.06 ± 0.19 vs WT 0.54 ± 0.20 $p=0.3077$; vs. $C3aR^{-/-}$
678 0.75 ± 0.20 $p=0.6302$; WT vs. $C3aR^{-/-}$ $p=0.8528$ and far; $C3^{-/-}$ 5.11 ± 0.63 vs WT
679 2.17 ± 0.30 $p=0.0001$, vs. $C3aR^{-/-}$ 2.60 ± 0.56 $p=0.0019$, WT vs. $C3aR^{-/-}$ $p=0.7646$. **(F)**
680 Total trials completed across sessions. Close WT 82.67 ± 9.60 , $C3^{-/-}$ 142.78 ± 11.31 ,
681 $C3aR^{-/-}$ 67.70 ± 11.75 ; Far WT 89.08 ± 9.16 , $C3^{-/-}$ 153.56 ± 12.60 , $C3aR^{-/-}$ 89.60 ± 16.73 .
682 Main effect of GENOTYPE; $F_{(2,28)}=10.6$, $p=0.0004$ [*posthoc* $C3^{-/-}$ vs WT $p=0.0015$;
683 vs. $C3aR^{-/-}$ $p=0.0007$; WT vs. $C3aR^{-/-}$ $p=0.8877$]. **(G)** The number of perseverative
684 errors (incorrect responses made after a reversal) were calculated and adjusted to
685 account for differences in the number of criteria reached per animal. Planned
686 comparisons at close; $C3^{-/-}$ 27.64 ± 4.52 , vs. WT 10.71 ± 3.09 $p=0.0008$, vs. $C3aR^{-/-}$
687 15.07 ± 3.34 $p=0.0142$; and far $C3^{-/-}$ 10.91 ± 1.32 , vs. WT 7.81 ± 1.09 ; $p=0.6512$, vs.
688 $C3aR^{-/-}$ 13.30 ± 3.11 $p=0.8060$. **(H)** Latencies of correct and incorrect responses.

689 Correct response latencies; main effect of SEPARATION $F_{(1,28)}=13.9$, $p=0.0009$;
690 Incorrect response latencies; main effect of SEPARATION $F_{(1,28)}=18.3$, $p=0.0002$.
691 Planned comparison of correct responses at close $C3^{-/-}$ 6.35 ± 0.95 s, vs. WT
692 11.42 ± 2.35 s; $p=0.1126$; vs. $C3aR^{-/-}$ 13.16 ± 1.95 $p=0.0295$; WT vs. $C3aR^{-/-}$ $p=0.7531$
693 and incorrect responses at close $C3^{-/-}$ 5.57 ± 0.68 s, vs. WT 15.62 ± 3.01 s; $p=0.0011$;
694 vs. $C3aR^{-/-}$ 13.66 ± 2.52 $p=0.0133$; WT vs. $C3aR^{-/-}$ $p=0.7278$. **(I)** Touches made to the
695 screen in the inter-trial interval (ITI). Planned comparisons at close; $C3^{-/-}$ 11.86 ± 2.13
696 s, vs. WT 4.96 ± 1.22 s; $p=0.0073$; vs. $C3aR^{-/-}$ 3.83 ± 1.03 $p=0.0025$; WT vs. $C3aR^{-/-}$
697 $p=0.8558$; and far $C3^{-/-}$ 13.22 ± 1.98 , vs. WT 5.83 ± 1.26 s; $p=0.0039$, vs. $C3aR^{-/-}$
698 6.63 ± 1.75 $p=0.0150$; WT vs. $C3aR^{-/-}$ $p=0.9267$. Data are mean \pm S.E.M. $N=12$ wildtype
699 animals, $N=9$ $C3^{-/-}$ animals and $N=10$ $C3aR^{-/-}$ animals. *, ** and *** = $p\leq 0.05$, $p\leq 0.01$
700 and $p\leq 0.001$ for *post-hoc* genotype comparisons respectively.

701

702

703

704

705

706

707

708

709

710

711

712

713

714

715 **4. Discussion**

716 Using knockout mouse models, we conducted an investigation of the impact of
717 signalling through the C3a/C3aR axis on adult hippocampal neurogenesis and
718 demonstrated separable effects of these proteins in regulating cellular, morphological
719 and functional aspects of neurogenesis. C3 impacted upon the survival and migration
720 of new neurons in the GCL, and while both C3 and C3aR influenced the morphology
721 of immature neurons, the effect was most evident in the total absence of C3aR
722 signalling. Lack of C3aR enhanced pattern separation without influencing other
723 aspects of cognition probed in the discrimination task, whereas the increased
724 neurogenesis and altered migration seen in *C3^{-/-}* mice was associated with
725 impairments in cognitive flexibility under conditions placing demands upon pattern
726 separation.

727 Our findings of enhanced survival in absence of C3 align with a prior report
728 focusing on C3d/CR2 signalling³⁶. Consideration of these findings alongside ours may
729 provide clues as to the specific pathways responsible for C3 effects upon cell survival.
730 Moriyama et al (2011)³⁶ demonstrated an inhibitory role for the C3d/CR2 axis in AHN,
731 reporting increases in immature GCs (BrdU⁺ NeuN⁺) in *CR2^{-/-}* mice using a pulse-
732 chase paradigm equivalent to our own. Our observation of increased basal
733 neurogenesis in *C3^{-/-}* mice but not *C3aR^{-/-}* mice is consistent with this since C3d is
734 derived from C3, thus *C3^{-/-}* mice lack C3d/CR2 signalling whereas *C3aR^{-/-}* mice do not.
735 This suggests that the survival effects we have seen may be due to a lack of signaling
736 through CR2, which under physiological conditions is expressed on neural progenitor
737 cells³⁶. Since other C3 breakdown products and their receptors, including
738 C5a/C5aR⁵⁷, C3b/CR3³⁶ and according to our data C3a/C3aR, do not modulate net

739 levels of adult neurogenesis³⁶, it is likely that C3d/CR2 signalling constitutes a novel
740 immune mechanism to maintain homeostatic levels of neurogenesis.

741 Our findings seem at odds with another report which showed a positive role for
742 the C3a/C3aR axis in regulating adult neurogenesis, evidenced by reduced numbers
743 of neural progenitors (BrdU⁺ DCX⁺ cells) and committed immature GCs (BrdU⁺ NeuN⁺)
744 in both C3^{-/-} and C3aR^{-/-} mice and wildtype mice treated with a C3aR antagonist³⁵.
745 While we did see a significant decrease in BrdU⁺ DCX⁺ cells in C3aR^{-/-} mice compared
746 to wildtypes, this was not seen in C3^{-/-} mice and our main finding of increased
747 neurogenesis (BrdU⁺ NeuN⁺ cells) is inconsistent with these results. However, the use
748 of different pulse-chase intervals in the previous study makes interpretation
749 challenging in terms of disentangling their effects on early progenitor proliferation
750 dynamics versus our effects on neuronal survival. Moreover, a subsequent study from
751 the same group using C3a-overpressing mice did not support a positive role for
752 C3a/C3aR signalling in regulating basal neurogenesis⁵⁷. Instead, our work using both
753 a short-term and a long-term labelling procedure permits clear dissociation of effects
754 on acute proliferation versus long-term survival, demonstrating a prominent role for C3
755 fragments in negatively regulating survival without affecting proliferation or neuronal
756 lineage commitment.

757 The mechanisms through which C3 may influence cell survival are unclear.
758 Only a small percentage of newborn cells are incorporated into the hippocampal
759 circuitry and ~70% are eliminated at the immature neuron stage^{61,62} via apoptosis-
760 coupled microglial phagocytosis. One possibility is that C3 signalling promotes
761 programmed cell death, either via cell-intrinsic or extrinsic mechanisms. Similar
762 mechanisms have been described for other complement factors implicated in
763 developmental neurogenesis⁸⁷. Another possibility relates to opportunities for synaptic

764 integration. During development, programmed cell death is necessary for optimal
765 matching of the neuronal population with available synaptic targets⁵⁸ and this is
766 recapitulated within the adult neurogenic niche, where important determinants of
767 survival include the success of immature GCs in forming synaptic contacts within the
768 molecular layer. Increased synapse density has been found in this area of the $C3^{-/}$
769 brain^{38,59}, presumably due to the absence of normal complement-mediated
770 developmental synaptic elimination²³. It is therefore possible that increased survival of
771 newborn cells in $C3^{-/}$ mice is facilitated by increased availability of synaptic contacts,
772 less competition and greater opportunity for integration and survival. The accelerated
773 migration of BrdU-labelled cells we observed in $C3^{-/}$ mice is consistent with this
774 notion, since migration into the GCL permits maturation via further reaching synaptic
775 contacts⁵³.

776 We also demonstrated effects of C3 and C3aR on the morphological complexity
777 of neuronal progenitor cells. Our results, showing reduced dendritic arborisation
778 primarily in the absence of C3aR, support prior *in vitro* studies implicating a necessary
779 role for C3aR in normal neuronal morphology^{39,42,43} and is the first to demonstrate this
780 relationship is maintained *in vivo*, within the adult neurogenic niche. While these
781 previous studies have mostly focused on either inhibition of C3aR, or addition of C3a,
782 the fact that our effects were most pronounced in the absence of C3aR suggests
783 redundancy of C3a in mediating morphological development. One possible
784 explanation is that VGF-deprived peptide TLQP-21, a known C3aR ligand^{60,61},
785 contributes to the maturation of immature neurons in the hippocampal neurogenic
786 niche, and further investigations are required to address this possibility. Interestingly,
787 we found effects of C3/C3aR on the morphology of neurons in the suprapyramidal, but
788 not infrapyramidal blade. How such specificity might come about is unclear and there

789 is scarce information relating to the transverse hippocampal axis. In a small number
790 of studies that have examined the two blades, differential neurogenesis, in addition to
791 connectivity, dendritic tree size and synapse density of GC neurons has been
792 demonstrated⁶²⁻⁶⁴. Functionally, although suprapyramidal GCs are known to respond
793 preferentially to spatial exploration^{65,66}, how their morphology contributes to the
794 functional properties of immature neurons in encoding spatial information is unknown.

795 To assess whether the changes we observed in AHN were associated with
796 functional changes in pattern separation, we used an established discrimination task
797 previously utilised to detect changes in pattern separation after pro-neurogenic⁴⁴ and
798 anti-neurogenic manipulations^{10,12,49}. Typically, enhancing adult neurogenesis is
799 associated with improved ability to discriminate highly similar stimuli or contexts^{44,67,68}
800 although this has not been entirely consistent across the literature^{69,70}. Despite
801 increased levels of neurogenesis, $C3^{-/-}$ mice showed impairments in spatial
802 discrimination performance, but only post-reversal, indicating impairments in cognitive
803 flexibility as opposed to pattern separation per se. Interestingly, it has been reported
804 that manipulations of neurogenesis only affected performance on trials after a learned
805 discrimination was reversed, rather than during the initial spatial discrimination¹⁴.
806 Additionally, abnormally enhanced neurogenesis in $C3^{-/-}$ mice may be responsible for
807 impairments in cognitive flexibility. Consistent with our data in $C3^{-/-}$ mice showing
808 elevated levels of neurogenesis alongside impaired reversal learning in the face of
809 increased spatial discrimination demands, ablating neurogenesis has led to
810 improvements in spatial working memory when animals were required to discriminate
811 highly similar cues presented in short succession or when animals needed to suppress
812 conflicting responses⁷¹, conditions akin to our task.

813 Despite the impaired performance of $C3^{-/-}$ mice in the reversal element of the
814 task, $C3^{-/-}$ mice paradoxically achieved the greatest number of criteria (and thus
815 reversals) across groups. We believe this is an epiphenomenon due to these mice
816 completing a greater number of trials throughout training and probe trials. These mice
817 therefore had more opportunity than other groups to reach criterion, even if achieved
818 in a less efficient manner. In the absence of a general hyperactivity phenotype, this
819 may indicate changes in motivation for reward. Moreover, decreased response
820 latencies and increased inappropriate responding in $C3^{-/-}$ indicated a failure of
821 behavioural inhibition and a potential impulsivity phenotype. It is unlikely that
822 increased speed of responding was due to a decreased perceived difficulty of the task
823 for these animals, given that their accuracy of responding was not improved. Using
824 tasks designed to specifically probe the influence of C3 on cognitive flexibility,
825 motivational behaviour and impulsivity will be a priority for future work.

826 $C3aR^{-/-}$ mice on the other hand were superior in their pattern separation ability
827 and were unimpaired by the reversal component of the task. If the cellular phenotypes
828 we have observed in these mice are linked to behavioural phenotypes, it seems
829 paradoxical that decreased morphological complexity of immature neurons in the
830 suprapyramidal blade would benefit function. Indeed, spatial learning has been shown
831 to increase dendritic complexity of immature neurons⁷². While it is known that younger
832 neural progenitor cells mediate pattern separation⁷³, it has also been demonstrated
833 that less morphologically complex immature DCX cells may be more important for
834 pattern separation and cognitive flexibility than more mature DCX cells and GC
835 neurons ($BrdU^+ NeuN^+$)⁷⁴. Additional factors likely of relevance include the fact that
836 C3aR is also part of a signalling pathway that mediates synaptic strength^{75,76} which
837 likely influences the synaptic connectivity both within and beyond the neurogenic

838 niche, consistent with evidence of altered cognition in *C3aR*^{-/-} mice from a variety of
839 contexts^{26,39,77,78}.

840 An important consideration is our use of constitutive knockouts. Knocking out
841 complement components such as C1q, C3 or CR3 results in sustained deficits in
842 synaptic connectivity^{23,33,38,79} which may alter the wider environment in which adult
843 neurogenesis takes place. Furthermore, increased neurogenesis is not always
844 beneficial and is often associated with abnormal neuronal maturation, integration⁸⁰
845 and migration, as we have seen. Therefore, despite the increased levels of
846 neurogenesis we report in *C3*^{-/-} mice, it is possible that their surplus adult born neurons
847 integrate into altered hippocampal circuit and this may have greater effects on
848 cognition than the impacts on GC survival per se.

849 Limitations of our study include our initial focus on male subjects due to known
850 fluctuations in AHN attributable to sex hormones⁸¹. Given important sexual
851 dimorphism in hippocampal cognition⁸² and complement activity⁴⁸, this will be a priority
852 in our future work. Finally, we had to adapt our analysis of the location discrimination
853 task due to the considerable difficulty subjects experienced in reaching criterion within
854 a single session, a known challenge of this task when applied in mice as opposed to
855 rats^{10,12,44,49}. Instead, we analysed performance across rather than within sessions of
856 each condition and as such there is likely to be more variability in our data introduced
857 by delays between individual sessions than in some other reports^{10,12,44,49}.

858 In conclusion, we show novel, negative regulatory roles for complement C3 and
859 C3aR in the survival and morphology of adult born neurons in the adult hippocampus,
860 findings consistent with the detrimental impact of excessive inflammation on
861 neurogenesis in neuropathologies such as temporal lobe epilepsy, where complement
862 activation is associated with chronically reduced neurogenesis⁸³⁻⁸⁵. We demonstrate

863 for the first time that C3 and C3aR influence neurogenesis-associated cognitive
864 processes of relevance to a range of neuropsychiatric disorders in which abnormal
865 neurogenesis and complement activity are implicated^{28,86} and add to the growing body
866 of evidence literature demonstrating intriguing non-canonical roles of complement in
867 the brain.

868
869
870
871

Author contributions

872 The study was designed by LJW, TH, BPM, MZ, WPG and LSW. LJW and TH
873 performed behavioural experiments. Molecular analyses were performed by LJW, NH,
874 CE and OM. Data interpretation were carried out by LJW, JH, NH, TRH, MZ, BPM,
875 LSW, TH and WPG. The manuscript was drafted by LJW, TH, WPG and LSW. All
876 authors approved the final manuscript.

877

Acknowledgements

879 The authors thank Rhys Perry, Pat Mason, Helen Read and other staff at BIOSV for
880 their animal care and husbandry. We also thank Anastasia Mirza-Davies and Joanne
881 McCabe for their assistance with the project, as part of placement awards from
882 Wellcome Inspire and The British Immunological Society. This work was supported
883 by a Wellcome Trust Integrative Neuroscience PhD Studentship awarded to LJW
884 (099816/Z/12/Z), a Waterloo Foundation Early Career Fellowship awarded to LJW, a
885 Hodge Centre for Neuropsychiatric Immunology Seed Corn and Project grant awarded
886 to LJW and a Wellcome Trust Strategic Award 100202/Z/12/Z (DEFINE) held by the
887 Neuroscience and Mental Health Research Institute at Cardiff University.

888

889

890 **Competing financial interests**

891 The authors declare no competing financial interests.

892

893 **Materials and correspondence**

894 All data from this study are available from the corresponding authors upon reasonable
895 request.

896

897 **References**

898

899

- 900 1. Doetsch, F. A niche for adult neural stem cells. *Current Opinion in*
901 *Genetics & Development* **13**, 543–550 (2003).
- 902 2. Kempermann, G., Jessberger, S., Steiner, B. & Kronenberg, G.
903 Milestones of neuronal development in the adult hippocampus. *Trends*
904 *Neurosci.* **27**, 447–452 (2004).
- 905 3. Kuhn, H. G. Control of Cell Survival in Adult Mammalian Neurogenesis.
906 *Cold Spring Harbor Perspectives in Biology* (2015).
- 907 4. Ge, S. *et al.* GABA regulates synaptic integration of newly generated
908 neurons in the adult brain. *Nature* **439**, 589–593 (2006).
- 909 5. Anacker, C. & Hen, R. Adult hippocampal neurogenesis and cognitive
910 flexibility - linking memory and mood. *Nat. Rev.* **18**, 335–346 (2017).
- 911 6. Kheirbek, M. A. & Hen, R. Add neurons, subtract anxiety. *Sci. Am.* **311**,
912 62–67 (2014).
- 913 7. Kempermann, G. Functional significance of adult neurogenesis. *Current*
914 *Opinion in Neurobiology* **14**, 186–191 (2004).
- 915 8. Yassa, M. A. & Stark, C. E. L. Pattern separation in the hippocampus.
916 *Trends Neurosci.* **34**, 515–525 (2011).
- 917 9. Schmidt, B., Marrone, D. F. & Markus, E. J. Disambiguating the similar:
918 The dentate gyrus and pattern separation. *Behav. Brain Res.* **226**, 56–65
919 (2012).
- 920 10. Clelland, C. D. *et al.* A functional role for adult hippocampal neurogenesis
921 in spatial pattern separation. *Science* **325**, 210–213 (2009).
- 922 11. Tronel, S. *et al.* Adult-born dentate neurons are recruited in both spatial
923 memory encoding and retrieval. *Hippocampus n/a–n/a* (2015).
924 doi:10.1002/hipo.22468
- 925 12. Coba, M. P. *et al.* TNiK is required for postsynaptic and nuclear signaling
926 pathways and cognitive function. *J. Neurosci.* **32**, 13987–13999 (2012).
- 927 13. Garthe, A., Roeder, I. & Kempermann, G. Mice in an enriched
928 environment learn more flexibly because of adult hippocampal
929 neurogenesis. *Hippocampus* (2015). doi:10.1002/hipo.22520

- 930 14. Swan, A. A. *et al.* Characterization of the role of adult neurogenesis in
931 touch-screen discrimination learning. *Hippocampus* **24**, 1581–1591
932 (2014).
- 933 15. Anacker, C. & Hen, R. Adult hippocampal neurogenesis and cognitive
934 flexibility — linking memory and mood. *Nat. Rev.* **18**, 335–346 (2017).
- 935 16. Burghardt, N. S., Park, E. H., Hen, R. & Fenton, A. A. Adult-born
936 hippocampal neurons promote cognitive flexibility in mice. *Hippocampus*
937 **22**, 1795–1808 (2012).
- 938 17. Seib, D. R., Espinueva, D. F., Floresco, S. B. & Snyder, J. S. A role for
939 neurogenesis in probabilistic reward learning. *Behavioral Neuroscience*
940 **134**, 283–295 (2020).
- 941 18. Ekdahl, C. T., Claasen, J.-H., Bonde, S., Kokaia, Z. & Lindvall, O.
942 Inflammation is detrimental for neurogenesis in adult brain. *Proc. Natl.*
943 *Acad. Sci. U.S.A.* **100**, 13632–13637 (2003).
- 944 19. Monje, M. L., Toda, H. & Palmer, T. D. Inflammatory blockade restores
945 adult hippocampal neurogenesis. *Science* **302**, 1760–1765 (2003).
- 946 20. Morley, B. J. & Walport, M. J. *The Complement FactsBook*. (Academic
947 Press, 1999).
- 948 21. Sayah, S., Ischenko, A. M., Zhakhov, A., Bonnard, A.-S. & Fontaine, M.
949 Expression of Cytokines by Human Astrocytomas Following Stimulation
950 by C3a and C5a Anaphylatoxins. *Journal of Neurochemistry* **72**, 2426–
951 2436 (2002).
- 952 22. Coulthard, L. G. & Woodruff, T. M. Is the Complement Activation Product
953 C3a a Proinflammatory Molecule? Re-evaluating the Evidence and the
954 Myth. *J. Immunol.* **194**, 3542–3548 (2015).
- 955 23. Stevens, B. *et al.* The classical complement cascade mediates CNS
956 synapse elimination. *Cell* **131**, 1164–1178 (2007).
- 957 24. Gorelik, A. *et al.* Developmental activities of the complement pathway in
958 migrating neurons. *Nature Communications* **8**, 15096 (2017).
- 959 25. Hong, S. *et al.* Complement and microglia mediate early synapse loss in
960 Alzheimer mouse models. *Science* **352**, 712–716 (2016).
- 961 26. Vasek, M. J. *et al.* A complement–microglial axis drives synapse loss
962 during virus-induced memory impairment. *Nature* **534**, 538–543 (2016).
- 963 27. Litvinchuk, A. *et al.* Complement C3aR Inactivation Attenuates Tau
964 Pathology and Reverses an Immune Network Deregulated in Tauopathy
965 Models and Alzheimer's Disease. *Neuron* **100**, 1337–1353.e5 (2018).
- 966 28. Kempermann, G., Krebs, J. & Fabel, K. The contribution of failing adult
967 hippocampal neurogenesis to psychiatric disorders. *Curr Opin Psychiatry*
968 **21**, 290–295 (2008).
- 969 29. Cho, K.-O. *et al.* Aberrant hippocampal neurogenesis contributes to
970 epilepsy and associated cognitive decline. *Nature Communications* **6**,
971 6606 (2015).
- 972 30. Das, T., Ivleva, E. I., Wagner, A. D., Stark, C. E. L. & Tamminga, C. A.
973 Loss of pattern separation performance in schizophrenia suggests
974 dentate gyrus dysfunction. *Schizophrenia Research* **159**, 193–197
975 (2014).
- 976 31. Gandy, K. *et al.* Pattern Separation: A Potential Marker of Impaired
977 Hippocampal Adult Neurogenesis in Major Depressive Disorder. *Frontiers*
978 *in Neuroscience* **11**, (2017).

- 979 32. Dohm-Hansen, S. & Johansson, M. Mnemonic discrimination of object
980 and context is differentially associated with mental health. *Neurobiology*
981 *of Learning and Memory* **173**, 107268 (2020).
- 982 33. Sekar, A. *et al.* Schizophrenia risk from complex variation of complement
983 component 4. *Nature* 1–17 (2016). doi:10.1038/nature16549
- 984 34. Harold, D. *et al.* Genome-wide association study identifies variants at
985 CLU and PICALM associated with Alzheimer's disease. *Nature Genetics*
986 **41**, 1088–1093 (2009).
- 987 35. Rahpeymai, Y. *et al.* Complement: a novel factor in basal and ischemia-
988 induced neurogenesis. *EMBO J* **25**, 1364–1374 (2006).
- 989 36. Moriyama, M. *et al.* Complement Receptor 2 Is Expressed in Neural
990 Progenitor Cells and Regulates Adult Hippocampal Neurogenesis.
991 *Journal of Neuroscience* **31**, 3981–3989 (2011).
- 992 37. Shi, Q. *et al.* Complement C3-Deficient Mice Fail to Display Age-Related
993 Hippocampal Decline. *Journal of Neuroscience* **35**, 13029–13042 (2015).
- 994 38. Perez-Alcazar, M. *et al.* Altered cognitive performance and synaptic
995 function in the hippocampus of mice lacking C3. *Experimental Neurology*
996 **253**, 154–164 (2013).
- 997 39. Lian, H., Li, Y., Lu, H.-C. & Zheng, H. NFκB-Activated Astroglial Release
998 of Complement C3 Compromises Neuronal Morphology and Function
999 Associated with Alzheimer's Disease. **85**, 101–115 (2015).
- 1000 40. Lledo, P.-M., Alonso, M. & Grubb, M. S. Adult neurogenesis and
1001 functional plasticity in neuronal circuits. *Nat Rev Neurosci* **7**, 179–193
1002 (2006).
- 1003 41. Stephan, A. H., Barres, B. A. & Stevens, B. The complement system: an
1004 unexpected role in synaptic pruning during development and disease.
1005 *Annu. Rev. Neurosci.* **35**, 369–389 (2012).
- 1006 42. Peterson, S. L., Nguyen, H. X., Mendez, O. A. & Anderson, A. J.
1007 Complement protein C1q modulates neurite outgrowth in vitro and spinal
1008 cord axon regeneration in vivo. *J. Neurosci.* **35**, 4332–4349 (2015).
- 1009 43. Shinjyo, N., Ståhlberg, A., Dragunow, M., Pekny, M. & Pekna, M.
1010 Complement-derived anaphylatoxin C3a regulates in vitro differentiation
1011 and migration of neural progenitor cells. *Stem Cells* **27**, 2824–2832
1012 (2009).
- 1013 44. Creer, D. J., Romberg, C., Saksida, L. M., van Praag, H. & Bussey, T. J.
1014 Running enhances spatial pattern separation in mice. *Proc. Natl. Acad.*
1015 *Sci. U.S.A.* **107**, 2367–2372 (2010).
- 1016 45. Paxinos, G. & Franklin, K. *Paxinos and Franklin's the mouse brain in*
1017 *stereotaxic coordinates.* (2019).
- 1018 46. Longair, M. H., Baker, D. A., Bioinformatics, J. A. 2011. Simple Neurite
1019 Tracer: open source software for reconstruction, visualization and
1020 analysis of neuronal processes. *Bioinformatics* **27**, 2453–2454 (2011).
- 1021 47. Garcia-Segura, L. M. & Perez-Marquez, J. A new mathematical function
1022 to evaluate neuronal morphology using the Sholl analysis. *J. Neurosci.*
1023 *Methods* **226**, 103–109 (2014).
- 1024 48. Hvoslef-Eide, M. *et al.* The touchscreen operant platform for testing
1025 working memory and pattern separation in rats and mice. *Nat Protoc* **8**,
1026 2006–2021 (2013).

- 1027 49. McTighe, S. M., Mar, A. C., Romberg, C., Bussey, T. J. & Saksida, L. M.
1028 A new touchscreen test of pattern separation: effect of hippocampal
1029 lesions. *Neuroreport* **20**, 881–885 (2009).
- 1030 50. Oomen. *et al.* The touchscreen operant platform for testing working
1031 memory and pattern separation in rats and mice. *Nat Protoc* **8**, 2006–
1032 2021 (2013).
- 1033 51. Horner, A. E. *et al.* The touchscreen operant platform for testing learning
1034 and memory in rats and mice. *Nat Protoc* **8**, 1961–1984 (2013).
- 1035 52. Wright, S. P. Adjusted P-Values for Simultaneous Inference. *Biometrics*
1036 **48**, 1005 (1992).
- 1037 53. Llorens-Martín, M., Rábano, A. & Ávila, J. The Ever-Changing
1038 Morphology of Hippocampal Granule Neurons in Physiology and
1039 Pathology. *Frontiers in Neuroscience* **9**, 4217–20 (2016).
- 1040 54. Zhao, C. Distinct Morphological Stages of Dentate Granule Neuron
1041 Maturation in the Adult Mouse Hippocampus. *Journal of Neuroscience*
1042 **26**, 3–11 (2006).
- 1043 55. Rahimi, O. & Claiborne, B. J. in *The Dentate Gyrus: A Comprehensive*
1044 *Guide to Structure, Function, and Clinical Implications* **163**, 167–181
1045 (Elsevier, 2007).
- 1046 56. Bussey, T. J. *et al.* The touchscreen cognitive testing method for rodents:
1047 How to get the best out of your rat. *Learn. Mem.* **15**, 516–523 (2008).
- 1048 57. Bogestål, Y. R. *et al.* Signaling through C5aR is not involved in basal
1049 neurogenesis. *J. Neurosci. Res.* **85**, 2892–2897 (2007).
- 1050 58. Buss, R. R., Sun, W. & Oppenheim, R. W. Adaptive roles of programmed
1051 cell death during nervous system development. *Annu. Rev. Neurosci.* **29**,
1052 1–35 (2006).
- 1053 59. Salter, E. W. *et al.* Complement C3-dependent glutamatergic synapse
1054 elimination in the developing hippocampus is region- and synapse-
1055 specific. *Preprint on BioRxiv* <https://doi.org/10.1101/2020.05.20.106930>
- 1056 60. Cero, C. *et al.* The TLQP-21 peptide activates the G-protein-coupled
1057 receptor C3aR1 via a folding-upon-binding mechanism. *Structure* **22**,
1058 1744–1753 (2014).
- 1059 61. Hannedouche, S. *et al.* Identification of the C3a Receptor (C3AR1) as the
1060 Target of the VGF-derived Peptide TLQP-21 in Rodent Cells. *Journal of*
1061 *Biological Chemistry* **288**, 27434–27443 (2013).
- 1062 62. Snyder, J. S., Ferrante, S. C. & Cameron, H. A. Late Maturation of Adult-
1063 Born Neurons in the Temporal Dentate Gyrus. *PLoS ONE* **7**, e48757–8
1064 (2012).
- 1065 63. Rahimi, O. & Claiborne, B. J. Morphological development and maturation
1066 of granule neuron dendrites in the rat dentate gyrus. *Prog. Brain Res.*
1067 **163**, 167–181 (2007).
- 1068 64. Scharfman, H. E., Sollas, A. L., Smith, K. L., Jackson, M. B. & Goodman,
1069 J. H. Structural and functional asymmetry in the normal and epileptic rat
1070 dentate gyrus. *Journal of Comparative Neurology* **454**, 424–439 (2002).
- 1071 65. Chawla, M. K. *et al.* Sparse, environmentally selective expression of Arc
1072 RNA in the upper blade of the rodent fascia dentata by brief spatial
1073 experience. *Hippocampus* **15**, 579–586 (2005).
- 1074 66. Ramírez-Amaya, V. *et al.* Spatial exploration-induced Arc mRNA and
1075 protein expression: evidence for selective, network-specific reactivation.
1076 *J. Neurosci.* **25**, 1761–1768 (2005).

- 1077 67. Sahay, A. *et al.* Increasing adult hippocampal neurogenesis is sufficient
1078 to improve pattern separation. *Nature* **472**, 466–470 (2011).
- 1079 68. Tronel, S. *et al.* Adult-born neurons are necessary for extended
1080 contextual discrimination. *Hippocampus* **22**, 292–298 (2010).
- 1081 69. Cameron, H. A. & Glover, L. R. Adult neurogenesis: beyond learning and
1082 memory. *Annu Rev Psychol* **66**, 53–81 (2015).
- 1083 70. Groves, J. O. *et al.* Ablating adult neurogenesis in the rat has no effect on
1084 spatial processing: evidence from a novel pharmacogenetic model. *PLoS*
1085 *Genet* **9**, e1003718 (2013).
- 1086 71. Saxe, M. D. *et al.* Paradoxical influence of hippocampal neurogenesis on
1087 working memory. *Proc. Natl. Acad. Sci. U.S.A.* **104**, 4642–4646 (2007).
- 1088 72. Tronel, S. *et al.* Spatial learning sculpts the dendritic arbor of adult-born
1089 hippocampal neurons. *Proc. Natl. Acad. Sci. U.S.A.* **107**, 7963–7968
1090 (2010).
- 1091 73. Nakashiba, T. *et al.* Young Dentate Granule Cells Mediate Pattern
1092 Separation, whereas Old Granule Cells Facilitate Pattern Completion.
1093 *Cell* **149**, 188–201 (2012).
- 1094 74. Webler, R. D., Fulton, S., Perera, T. D. & Coplan, J. D. Maturation
1095 phase of hippocampal neurogenesis and cognitive flexibility.
1096 *Neuroscience Letters* **711**, 134414 (2019).
- 1097 75. Lian, H. *et al.* NFκB-Activated Astroglial Release of Complement C3
1098 Compromises Neuronal Morphology and Function Associated with
1099 Alzheimer’s Disease. **85**, 101–115 (2015).
- 1100 76. Stokowska, A. *et al.* Complement peptide C3a stimulates neural plasticity
1101 after experimental brain ischaemia. *academic.oup.com*
1102 doi:10.1093/brain/aww314
- 1103 77. Coulthard, L. G., Hawksworth, O. A., Conroy, J., Lee, J. D. & Woodruff, T.
1104 M. Complement C3a receptor modulates embryonic neural progenitor cell
1105 proliferation and cognitive performance. *Molecular Immunology* **101**,
1106 176–181 (2018).
- 1107 78. Pozo-Rodríguez, A., Ollaranta, R., Skoog, J., Pekny, M. & Pekna, M.
1108 Hyperactive Behavior and Altered Brain Morphology in Adult Complement
1109 C3a Receptor Deficient Mice. *Front. Immunol.* **12**, 604812 (2021).
- 1110 79. Schafer, D. P. *et al.* Microglia sculpt postnatal neural circuits in an activity
1111 and complement-dependent manner. *Neuron* **74**, 691–705 (2012).
- 1112 80. Scharfman, H. E. & Hen, R. NEUROSCIENCE: Is More Neurogenesis
1113 Always Better? *Science* **315**, 336–338 (2007).
- 1114 81. Mahmoud, R., Wainwright, S. R. & Galea, L. A. M. Sex hormones and
1115 adult hippocampal neurogenesis: Regulation, implications, and potential
1116 mechanisms. *Frontiers in Neuroendocrinology* **41**, 129–152 (2016).
- 1117 82. Yagi, S. & Galea, L. A. M. Sex differences in hippocampal cognition and
1118 neurogenesis. *Neuropsychopharmacology* 1–14 (2018).
1119 doi:10.1038/s41386-018-0208-4
- 1120 83. Hattiangady, B., Rao, M. & Shetty, A. Chronic temporal lobe epilepsy is
1121 associated with severely declined dentate neurogenesis in the adult
1122 hippocampus. *Neurobiol. Dis.* **17**, 473–490 (2004).
- 1123 84. Aronica, E. *et al.* Complement activation in experimental and human
1124 temporal lobe epilepsy. *Neurobiol. Dis.* **26**, 497–511 (2007).

- 1125 85. Jamali, S. *et al.* Large-scale expression study of human mesial temporal
1126 lobe epilepsy: evidence for dysregulation of the neurotransmission and
1127 complement systems in the entorhinal cortex. *Brain* **129**, 625–641 (2006).
1128 86. DeCarolis, N. A. & Eisch, A. J. Hippocampal neurogenesis as a target for
1129 the treatment of mental illness: A critical evaluation. *Neuropharmacology*
1130 **58**, 884–893 (2010).
1131 87. Bernard, M. *et al.* Characterization of C3a and C5a receptors in rat
1132 cerebellar granule neurons during maturation. Neuroprotective effect of
1133 C5a against apoptotic cell death. *J. Biol. Chem.* **279**, 43487-43496 (2004).